Radiographic Correlation in Orthopedic Pathology

Michael J. Klein, MD

Abstract: Radiographic correlation is an essential adjunct for the accurate diagnosis of orthopedic lesions, yet it is a skill neglected by pathologists. The purpose of this review is to demonstrate why performing this correlation is an essential part of the diagnostic process and not merely an interesting adjunct to the surgical pathology of orthopedic lesions. The relationships between x-rays and tissues are explored with an emphasis on bone and soft tissue composition and structure. In addition, the rudiments of complementary imaging studies and how to incorporate their data into diagnoses are examined.

Key Words: bone scintigraphy, bone tumors, CT scanning, magnetic resonance imaging, musculoskeletal imaging

(*Adv Anat Pathol* 2005;12:155–179)

At sometime during their training, pathologists are taught that radiographic correlation is necessary for the proper interpretation of bone histopathology. Whereas this has been true since x-rays were first used diagnostically, it was formally espoused in a concept Jaffe called the "tridimensional view."[1] In coining this term, Jaffe meant that the accurate diagnosis of bone lesions requires close communication between the pathologist, radiologist, and orthopedic surgeon. It has been suggested that this approach results in the correct diagnosis 95% of the time.[2] Because very few attending pathologists in residency programs have had training in radiology or in orthopaedics and because it is rare for pathology residents to have the time and access for such training, it is difficult for a pathologist to acquire the skills necessary to meaningfully correlate radiographs and histology.

Since orthopedic tissues are deep-seated, they are essentially invisible without radiographic imaging. Diseases that alter the anatomy and physiology of these structures are similarly invisible, even to the orthopedic surgeon sampling them. Radiographs and their complementary ancillary imaging studies visualize the interaction of normal structures and their diseases. They give some indication not only how a disease alters normal structures, but also that normal structures affect the disease process. In some cases, they may even reveal why a disease is causing the presenting symptoms.

Bones are hard tissues; they are hard to biopsy, hard to process, and hard to interpret correctly. The use of vibrating saws and rapid decalcifying agents to which bone is relegated in many high-volume histology laboratories may add artifacts that make the inherent histologic difficulties even worse. Imaging provides a complete picture that not only sees the process as a whole, but also puts a biopsy in its proper perspective. Whereas some bone diseases are diagnosable with certainty on routine x-rays alone, when a lesion requires biopsy, a rudimentary understanding of imaging can help the pathologist assess whether the actual pathologic process has been sampled representatively.[3] It may even clarify whether what is in the section agrees with or does not agree with the context of what appears in the images.

The increasing workload of modern pathology laboratories combined with pressure from clinicians to make ever more rapid diagnoses imposes time and manpower demands of which we are all too familiar. These often prevent pathologists from wandering too far from the laboratory. On the other hand, it is often necessary to leave the laboratory to gain access to clinical images, especially when these have not been generated electronically. Even when the imaging studies can be easily and rapidly obtained, the pathologist needs some understanding of skeletal and soft tissue anatomy and its alterations in disease. Without this knowledge, a pathologist who finally manages to obtain imaging studies for a case is much like the barking dog that finally catches an automobile; when this happens, the dog usually cannot drive the vehicle. The less experience a pathologist has with radiographic correlation, the more important it is to have the help of a competent radiologist to help put the histologic findings in their proper context.

INTERACTIONS OF X-RAYS AND MUSCULOSKELETAL TISSUES

X-rays are high-energy electromagnetic waves of approximately one Angstrom in wavelength. Because they are high in energy and much narrower than atoms, they have the ability to analyze matter at its atomic level. Lord Rutherford's experiments defining the atomic nucleus established that the nuclear volume of any given atom is approximately one-billionth the volume of the entire atom.[4] Despite the apparent solidity of matter, the most essential atomic characteristic not apparent at the visual level is that most of an atom consists of the space between its electron orbitals and nuclei. Whereas nearly all of atomic mass (99.94%) is derived from its protons and neutrons, atomic space is due to the statistical locations of

Professor of Pathology, Head, Section of Surgical Pathology, The University of Alabama at Birmingham, Division of Anatomic Pathology, Birmingham, Alabama.

Reprints: Michael J. Klein, MD, Professor of Pathology, Head, Section of Surgical Pathology, The University of Alabama at Birmingham, Division of Anatomic Pathology, 3545 North Pavilion, 619 19th St. South, Birmingham, AL 35249-7331 USA (e-mail: mklein@path.uab.edu).

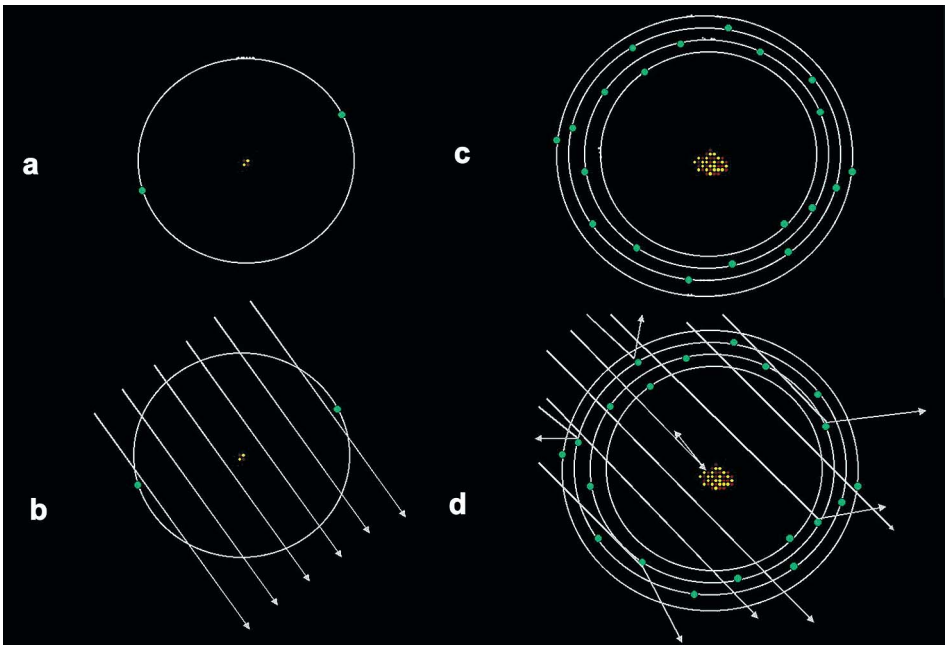

FIGURE 1. A–D, A and C are schematic representations of a helium atom with two electrons and one electron orbital and a calcium atom with 20 electrons and four orbitals respectively. In B and D, the same atoms are bombarded with x-rays to demonstrate the increasing statistical likelihood of x-ray absorption by electron capture and scatter. The diagrams do not account for inter-atomic spacing by helium, a noble gas. Although Figure 1D shows a putative blockade of an x-ray wave by the nucleus, the actual probability is less likely, because at the scale the nucleus is drawn, the outer electron orbital would measure 10.2 meters in diameter!

electrons. This means that if the space could be extracted from all atoms in an object, that object would occupy one-billionth of its customary three-dimensional space. Without intra-atomic space, the volume normally occupied by 5000 aircraft carriers (planes, crews, and fuel included) would comfortably fit inside a sphere about the size of a baseball, but it would be no different in total mass than the 5000 aircraft carriers (it would weigh the same). More extreme examples are actually found in nature as white dwarf stars, pulsars, and (theoretically) black holes.

The ability of x-rays to penetrate matter, then, is due to the presence of this space within atoms. Objects composed of elements with high atomic weights are radiodense because these elements contain a greater number of orbiting electrons, which are statistically more likely to absorb, scatter, or deflect x-ray energy than those with fewer electron orbitals. Whereas nuclei can absorb and deflect x-rays, nuclei occupy so little atomic volume (1×10^{-9}) that even in atoms with many nuclear particles (gold, lead, osmium, etc.) the nuclei play statistically no role in x-ray absorption (Fig. 1).

It should be obvious from this discussion that radiodensity also depends upon the physical property of intermolecular spacing. Whereas the atoms of krypton contain many more electrons than calcium atoms, for example, the native state of krypton is a gas. It is radiolucent because a gas has greater distances between its atoms than a liquid or a solid. Radiodensity is not dependent upon other certain other physical properties of matter. For instance, a diamond, which is the hardest substance on the Mohs hardness scale, is as radiolucent as graphite, the softest substance on the same scale. They are both composed of pure carbon, which has only six electrons in its atomic orbitals (Fig. 2A). A so-called cubic zirconia, one of the more common faux diamonds, is even more radiodense

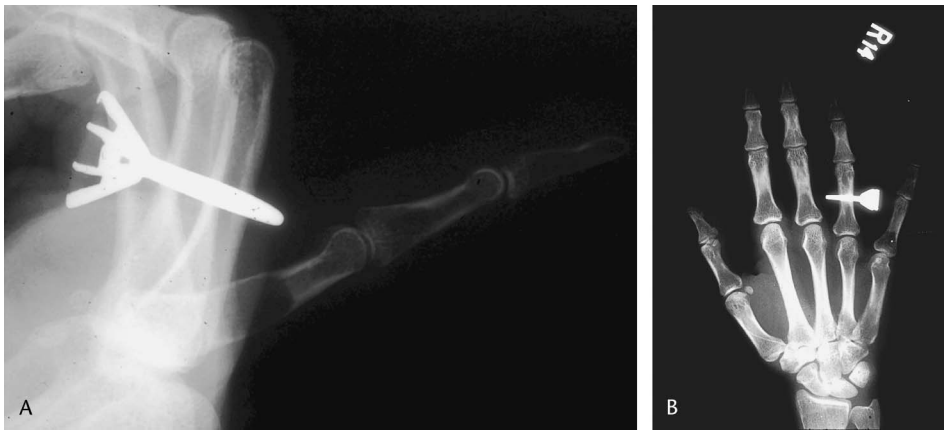

FIGURE 2. A, A 40-year-old woman had her hand x-rayed after suffering fifth finger pain after minor trauma. The film shows a slightly expansile, lucent lesion of the base of the fifth phalanx, which is an enchondroma with a nondisplaced fracture. It also demonstrates a very large, radiolucent marquis-shaped stone in a heavy metal (platinum) Tiffany setting. The radiolucency of the stone is compatible with carbon (element 6)—and therefore is probably a true diamond. B, A 50-year-old woman preferred to wear a ring with a costume stone for security reasons. The costume stone is a cubic Zirconic mainly comprised of Zirconium oxides. Zirconium has 40 electrons and 5 orbitales (versus 20 and 4 for calcium) so is radiodense.

than calcium because zirconium, the element of which most of its molecules are composed, not only possess more electrons than calcium but has an additional electron orbital (Fig. 2B).

Radiographs are produced when x-rays generated by a cathode ray tube are passed through a filter, a collimator, the patient, a grid, and a detector.[5] The x-ray tube produces a wide spectrum of electromagnetic waves; the filter, often consisting of a metal sheet, removes radiation below the desired energy lessening patient exposure and x-ray scatter, and the collimator focuses the x-ray beam.[5]

X-rays have the ability to sensitize a photographic emulsion, but they do so at a much slower rate than visible light because the reaction is photochemical and x-rays are in the wrong part of the electromagnetic spectrum to produce photographic energy. To accelerate this process, the photographic film used in x-rays is placed in a cassette, which has a fluorescent coating composed of rare earth compounds inside. X-rays striking this coating cause electrons to be raised to higher energy levels; when they return to their normal energy state, they give off secondary emissions of fluorescent light, which then strike the film, making a contact print inside the light tight cassette. Precipitation of silver in the emulsion takes place as a result of this secondary photochemical reaction, which results in exposure of the film.[6] Because fluorescence intensity is proportional to the incident x-ray intensity, radiodense objects, which absorb x-rays, prevent this radiation from being absorbed by the fluorescent coating.[5] The emulsion beneath these areas has very little silver precipitated. The result is that bones appear white on x-ray films. The converse is true for radiolucent objects, which appear dark.

Whereas conventional radiographs are actually large photographic negatives indirectly produced, there are at least three other types of ways to produce radiographs. In fluoroscopy, film is replaced by an image intensifier and a video camera, producing an image that can be viewed in real time and recorded. A third method makes use of multiple small x-ray detectors that can produce digital images directly to construct radiographs. Finally, photographic plates with light-sensitive phosphors can produce electrical charges proportional to the intensity of the incident light; lasers can translate this into digital pixels that can be stored on a computer.[5]

Even though radiodensity relates to elemental atomic structure, it is sometimes easier to think of the interaction of the body with x-rays in much the same way as the ancient Greeks thought of the composition of all matter as air, earth, fire, and water. In the case of living tissues, x-rays can be thought of as having four radiodensities: gas (air), fat, water, and bone (or calcium) in order of increasing radiodensity.

Whereas air, fat, and water are radiolucent and relatively dark on a conventional x-ray film, under certain circumstances they may be visualized because of contrast with adjacent tissues that are more radiodense. A prime example of this is the epiphyseal growth plate or the articular cartilage of the joints. Even though hyaline cartilage has the same relative radiodensity as water, the presence and position of a growth plate

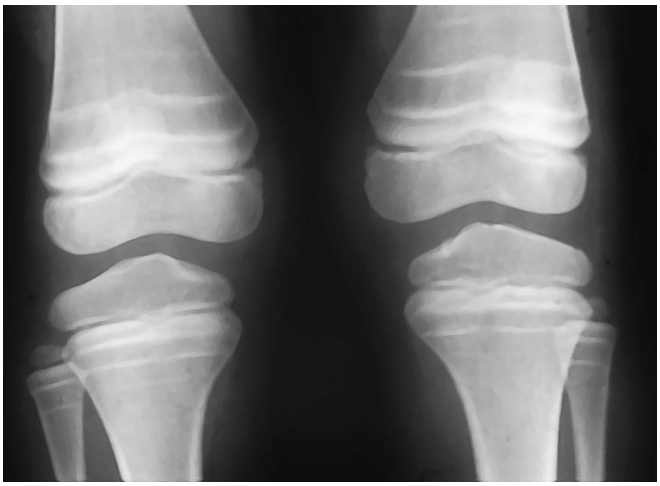

FIGURE 3. Bilateral knees in a child. Note the separation of the femurs and tibias consistent with thick articular cartilage. Note that the six growth plates are similarly dark between the bone ends. Note, in addition, that there are three radiodense lead lines in each of the six long bones pictured here. These lines are equally spaced bilaterally in the tibias and fibulas. They are equally spaced in the distal femurs, but the distance between lines is further apart in the femurs indicating faster differential growth in the femoral growth plates.

FIGURE 4. In this case of severe osteoarthritis of the left knee, there is practically no articular cartilage separating the lateral femoral condyle and tibial plateau (the dark joint space is narrowed). On the medial side, there is no joint space discernible and there are subarticular lucencies representing degenerative cysts.

can be ascertained because of the radiodense bone of the epiphysis and metaphysis surrounding it (Fig. 3).

The synovium and synovial fluid can not be distinguished from the hyaline cartilage in a normal joint, because the radiodensity of all these structures is water. On the other hand, changes in the adjacent ossified tissues surrounding a joint may be observed; alterations in the interposed soft tissues many then be evaluated indirectly. If there is destruction of articular cartilage, for example, the adjacent bony structures are usually more closely approximated and there may be secondary changes in the subarticular bone or at the bony margins of the joint ends (Fig. 4).

Even though a radiograph is a two-dimensional representation of a three-dimensional structure, this fact is easily forgotten. Pathologists easily interpolate microscopic images into three-dimensional constructs of their corresponding pathologic processes; they sometimes forget that radiographs must similarly be translated into three dimensions. A radiograph of a long bone such as the femur appears to have two whiter and more compact outer zones that correspond to the cortex and a hazier central portion between the compact zones corresponding to the medullary cavity. A three-dimensional construct without the surrounding soft tissues reminds us that because the cortex completely surrounds the long bone, the area

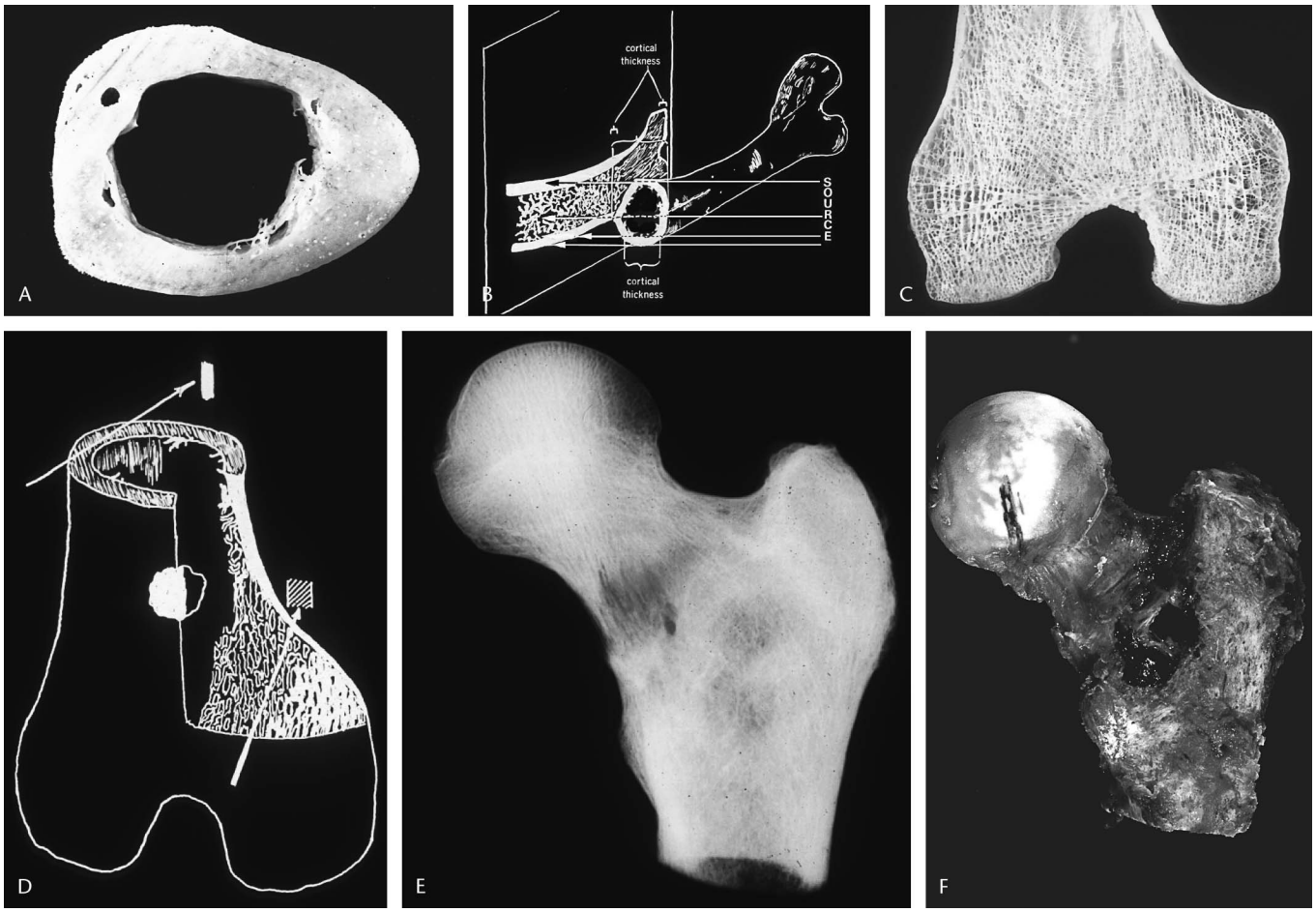

FIGURE 5. A, A cross section of compact bone from the femoral diaphysis demonstrating that virtually all bone mass is within the cortex and the medullary cavity is hollow once the marrow fat has been removed. B, A schematic representation of x-rays traversing the midshaft of a femur demonstrates that when the two-dimensional image is reconstructed in three dimensions, all of the x-rays traverse compact bone, but those traversing the outer cortex go through a thicker path of bone. What is perceived as the ''medulla'' is actually two compact layers plus marrow fat. C, A normal adult distal femur, macerated specimen with marrow removed demonstrates that most of the bone volume (of which 75% is marrow space), consists of cancellous bone; the cortex is comparatively thin. D, A schematic representation of the distal femur to demonstrate that in the diametaphyseal region most of the radiographic image is derived from cortical bone and in the metaphyseo-epiphyseal region most of the image is derived from cancellous bone. Lesions inside the medullary cavity that do not destroy more than 40% of the bone in the path of x-rays in that view are essentially invisible. Lesions that produce sclerosis are visible. E, A whole specimen radiograph of a proximal femur removed for metastatic renal cell carcinoma. Note that the bone shows some radiolucency above and below the intertrochanteric lines, but that the degree of lucency does not appear massive. F, Gross specimen from the same case demonstrates a complete lytic defect affecting the full cortical thickness of the anterior intertrochanteric line that extends halfway into the medullary cavity. One full cortex and more than half of the bone contents are destroyed by metastatic carcinoma.

corresponding to the medullary cavity is, in fact, composed of the medullary cavity plus the cortical layers anterior and posterior to the medullary cavity (Figs. 5A and 5B). We perceive the outer regions as more radiodense simply because the path the x-ray beam crosses in these parts of the bone is thicker than the sum of the cortices anterior and posterior to the medullary cavity. Most of that part of the image that we infer is medullary is actually produced by a stream of x-ray photons passing through two cortices and a medullary cavity that is composed almost entirely of fat; thus the image is essentially a cortical projection. Because of the differences in radiodensity between fat and compact bone, any lesion confined to the medullary cavity of the diaphysis that does not destroy the cortex is, for all practical purposes, invisible on a routine x-ray film.

Conventional x-rays are so insensitive that a purely destructive lesion must destroy at least 40% of the bone in the path of the x-ray beam to be appreciated. In a long bone, this amounts to the destruction of 80% of one cortical thickness in a single view. This relative insensitivity is an important reason why conventional radiographs are done in more than one view. Radiographs taken at right angles to one another more easily isolate lesions confined to one cortex or part of one cortex. Destructive lesions occurring in the ends of long bones, where cancellous bone is dominant in volume, also require the loss of 40% of bone volume in any given projection to be identified. On the other hand, lesions that contain calcifications or produce radiodense bone matrix tend to be additive with the bone radiodensities already present (Figs. 5C–5F) and may be visualized on a conventional radiograph even without much bone destruction.[7,8]

Additional factors may be confusing in routine radiographs. Because the image results from a photon beam projected through a subject onto a cassette or a radiation detector, those portions of the patient that face away from the recording device will be magnified in the image with respect to those parts that are closest to the recording device. Those portions of the subject that are more radiodense tend to appear more sharply in the final image than those that are more radiolucent. Some of the shadows and image blur that come from tissues with less radiodensity are produced by Compton scattering, a result of electrons absorbing energy and then giving off secondary high-energy photons at different angles than incident x-ray photons.[9]

Certain sources of variation in an x-ray film can be influenced by conditions that are technically controllable. For example, increasing the kilovoltage potential of the cathode ray tube will increase the penetration of x-rays, accentuating the osseous structures and causing overexposure of the soft tissue. Similar effects could be achieved if the exposure time at a given kilovoltage potential could be increased, although this is limited by the ability of a subject to remain stationary.[6,10]

STATISTICAL CONSIDERATIONS IN PATHORADIOLOGIC ANALYSIS

There are other considerations that must be taken into account when examining conventional bone radiographs. Because bone diseases tend to follow statistically reproducible patterns of age, skeletal distribution, and radiographic appearances, one should apply these same diagnostic parameters when examining radiographs.[7] Whereas a pathologist is often most concerned with identifying or ruling out the presence of

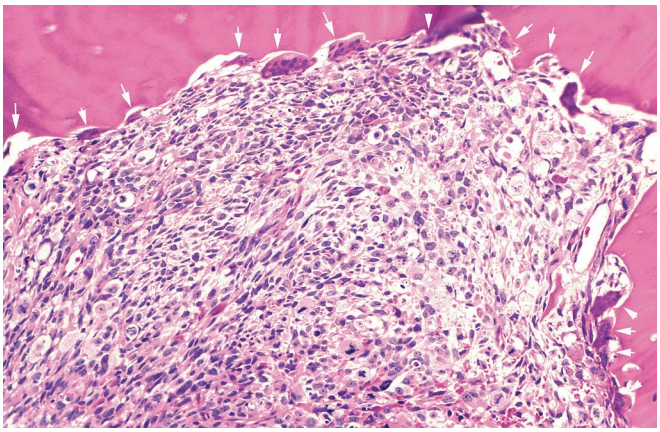

FIGURE 6. The interface of a radiolucent lesion and adjacent bone demonstrates that the cause for osteolysis is osteoclast activity at the edge of the lesion (arrows).

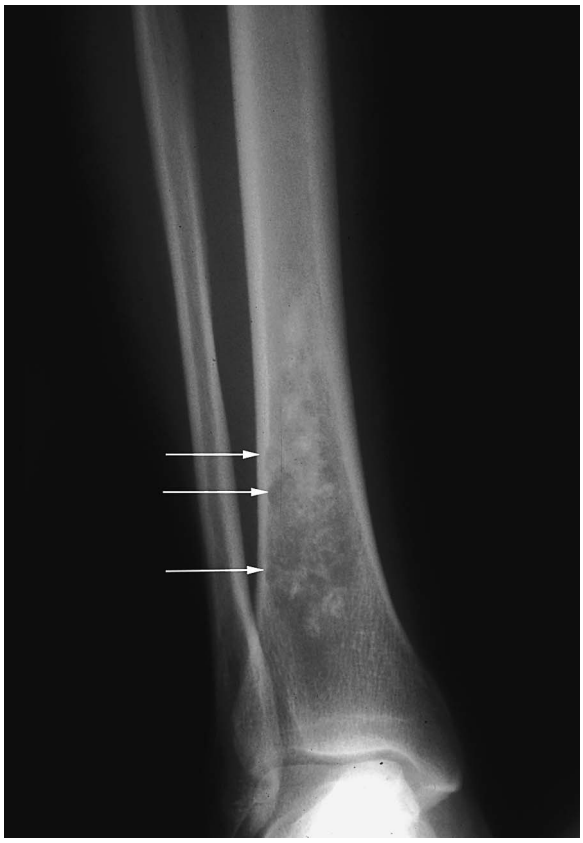

FIGURE 7. Routine x-ray of a distal tibia containing a large benign cartilage lesion (enchondroma). Note that in addition to calcified radiolucent matrix, there is scalloping of the lateral endosteal cortex (arrows).

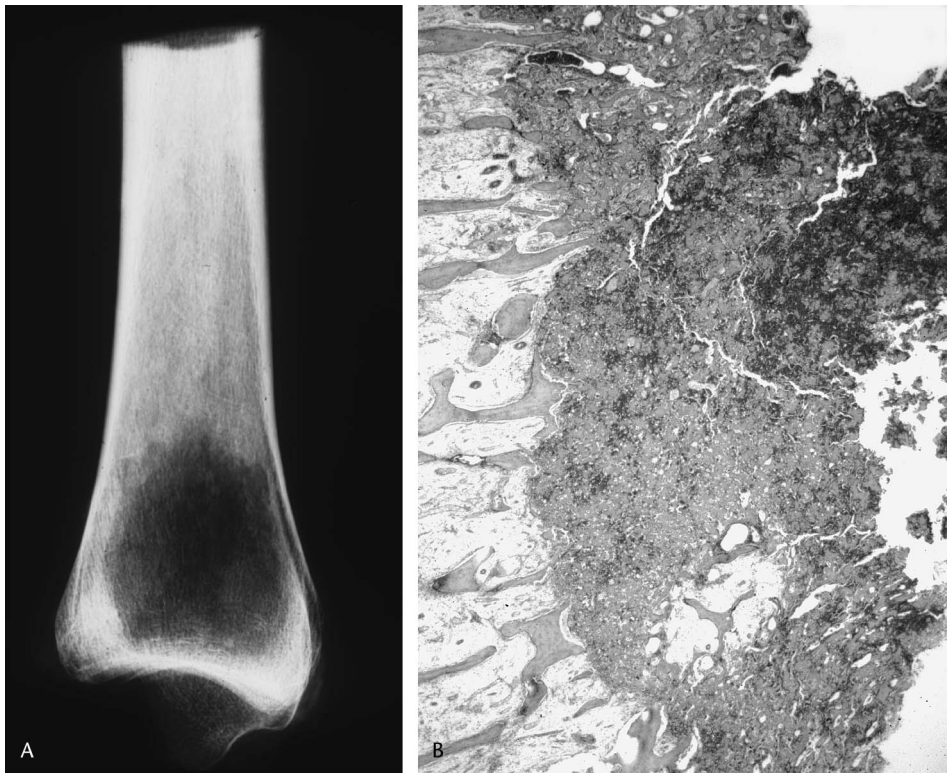

FIGURE 8. A, Specimen radiograph showing an idealized radiolucent lesion with geographic margins. The boundary between normal bone and lesional content is abrupt, signifying that there is little destruction or abnormality in the tissue bordering the lucent area. B, Interface of a tumor showing geographic radiolucency with adjacent bone on a radiograph. At low-power magnification, it is appreciated that in the area of the tumor (center and right) there is virtually no pre-existent bone whereas to the left of the tumor-bone interface, the bone and marrow are completely unremarkable.

neoplastic disease, tumors of bone are far outnumbered by developmental problems, infections, traumatic diseases, metabolic diseases, and degenerative diseases in almost every age group.

Congenital and developmental disorders are numerous in the first two decades of life and metabolic and degenerative diseases become more frequent with advancing age. Infections are also frequent at all ages, though they are usually hematogenous in the first two decades and related to trauma or peripheral vascular disease later in life. Traumatic diseases are frequent at all ages. When a neoplastic process is present, patient age is still a very important statistical consideration. Whereas primary malignant tumors such as osteosarcoma and Ewing sarcoma primarily affect young individuals, they are fairly uncommon before the second decade and rare after the third decade. Giant cell tumor and chondrosarcoma have a predilection for the mature skeleton. Metastatic carcinoma and plasma cell myeloma seldom affect the skeleton prior to the fifth decade.

The entire bone containing the lesion as well as the portion actually involved should be examined, because not only do certain lesions affect particular bones and particular parts of these bones, but they may also be multifocal. Clinically uninvolved bones should sometimes be examined radiographically, because metabolic diseases, which may mimic tumors, usually affect the entire skeleton to some extent. Other factors, such as whether a lesion is solitary or multifocal, involves the joint, or possesses features characteristic for matrix production are also important considerations. The presence of bone matrix, cartilage matrix, and fibrous tissue in a histologic section may direct one's thinking toward a bone tumor, but connective tissue matrix is much more frequently associated with a repair reaction at the periphery of fractures or infections, and sometimes within fibrous dysplasia.[8]

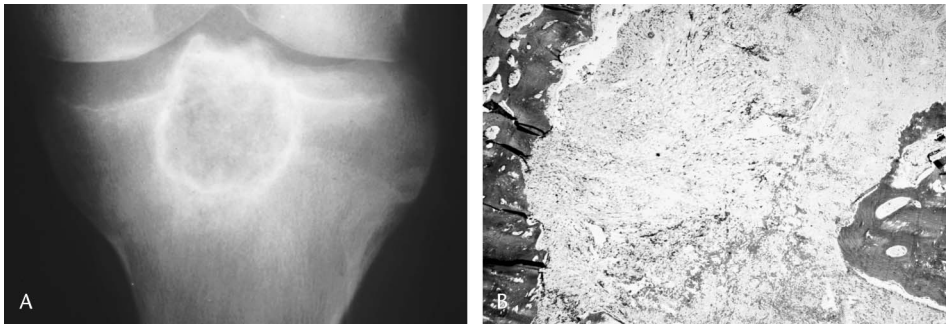

FIGURE 9. A, An anteroposterior radiograph of a proximal tibia with a marginated radiolucent lesion. Note the dense perilesional sclerosis representing new bone formation. B, Marginated lesion at low power. Surrounding the fibrous central part of this lesion, the bone has been slowly reconstructed and at least in part has the appearance of cortex.

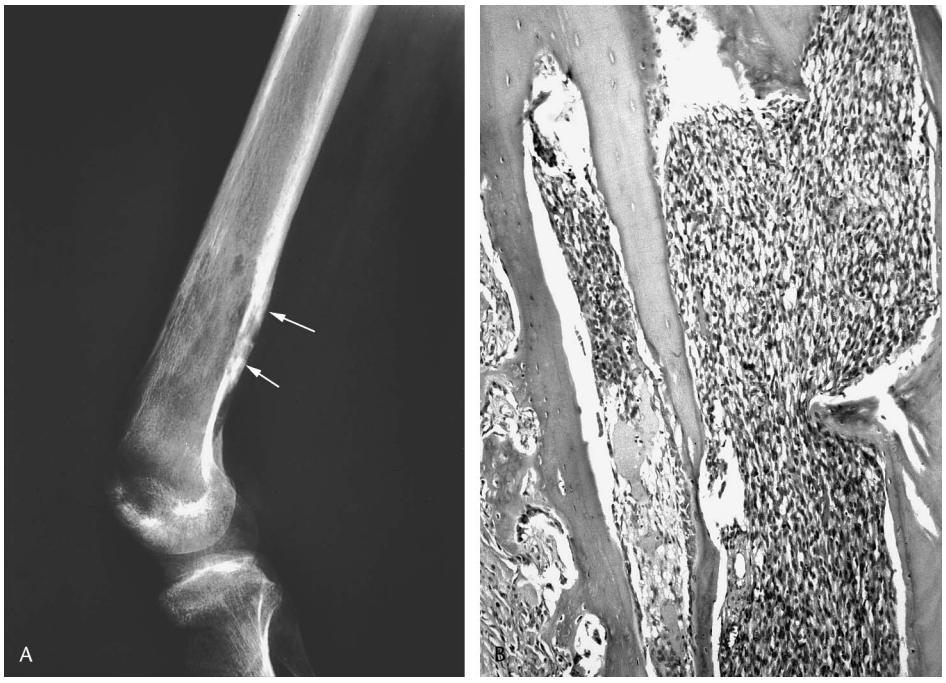

FIGURE 10. A, Lateral radiograph demonstrating a moth-eaten lesion of the distal and midfemur. This pattern suggests an aggressive lesion of at least low-grade malignancy. In this view it can be appreciated that a significant amount of cortical destruction is present from the confluent lenticular defects; the upper and lower boundaries of destruction are ill defined. The posterior cortical destruction is accompanied by periosteal new bone formation (arrows). B, A section taken through the cortex of this bone demonstrates a spindle cell lesion advancing within reabsorbing Haversian canals. There is some extension outside the cortex with periosteal reaction (lower left).

MAJOR CATEGORIES OF RADIOGRAPHIC LESIONS

The assessment of osseous lesions depends upon the consideration of the relationship between bone structure and the manner in which bone tissue responds to the presence of a pathologic process. In general, bone reacts to structural and functional abnormalities in the same way regardless of whether the lesion is traumatic, inflammatory, metabolic, or neoplastic; the variations in reaction are only of degree.[10] Osseous tissues react to a pathologic process by bone absorption, new bone production, or some combination of both.[11] The radiographic appearance is a result of the relative dominance of each process combined with the radiographic characteristics unique to the particular pathologic process. The final radiograph is merely a statistical analysis of these dynamic interrelationships at a given point in time.

Perhaps the most important radiographic characteristic by which to assess the biologic potential of a pathologic process is whether a border between lesional tissue and normal osseous tissue can be defined. The region between lesional and normal tissue is sometimes referred to as a "transition zone".[12] Generally, lesions that have better defined transition zones are less aggressive biologically. This is because whereas the forces that govern bone absorption may be complex, the process of

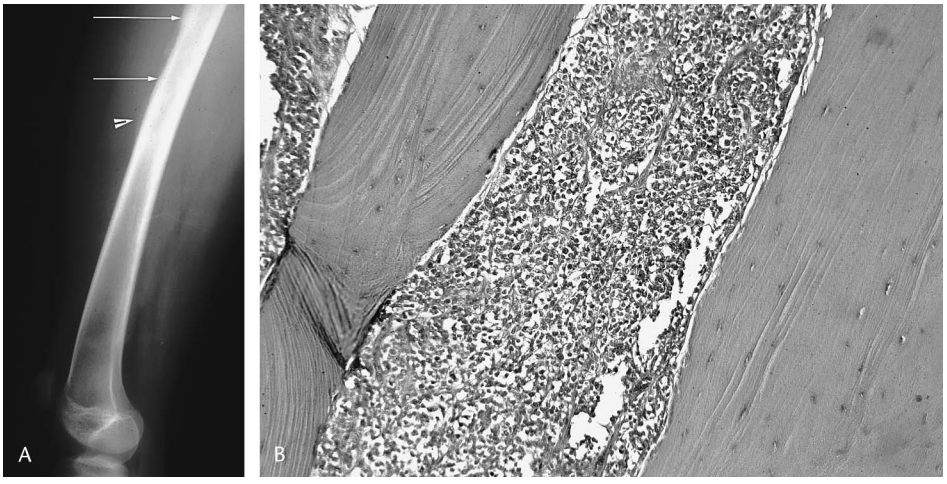

FIGURE 11. A, Permeative lesion of femur. The bone demonstrates no significant radiolucency, but there is a slight concave defect in the anterior cortex (between two arrows) associated with pressure erosion of the overlying soft tissue mass. There is an indistinct and incomplete periosteal reaction (arrowhead and beginning at upper arrow). The abnormal area within the bone has neither beginning nor end. B, Biopsy of cortex and endosteum of same bone seen in 11A demonstrates that even though the normal lamellar (mature) bone structure is present, all of the soft tissue interstices are completely filled with a small round cell tumor. The margins of the bone are smooth, indicating no evidence of osteoclast activity.

FIGURE 12. Anteroposterior radiograph demonstrating an intracortical abscess. Note well-circumscribed radiolucency with an associated fusiform medial cortical thickening, the result of slow periosteal irritation.

bone absorption is not a direct result of the pathologic process, but of its associated osteoclastic activity. Osteoclast recruitment from histocytic precursors and activation of extant osteoclasts takes time. A process indolent enough to produce a well-demarcated transition zone will not penetrate the intertrabecular marrow spaces of the cancellous bone adjacent to the advancing edge of the lesion to any great extent. Bone destruction by osteoclasts associated with these kinds of lesions tends to be confined to the area of the pathologic process itself (Fig. 6).

In the same way, a benign lesion pushing against the endosteal cortex may cause scalloped erosion of the inner cortex over a long time due to osteoclast activity along the endosteum (Fig. 7). Unless the cortex is devitalized, however, benign lesions do not usually penetrate the cortex nor extend into its vascular canals.

The radiologic appearance of a lesion is termed *geographic* if its transition zone is narrow and well defined.[13,14] This type of reaction implies that osteoclastic absorption of bone at the periphery of a lesion removes bone at approximately the same rate as the lesion enlarges within the bone. If a histologic section is taken in such a way as to examine the interface between the bone and the lesion, a fairly abrupt end to the lesion and interface with normal bone is observed (Figs. 8A and 8B).

A geographically circumscribed lesion may be described as *marginated* if there is a region of radiodensity at the interface of lesional and normal tissue.[15] This appearance is due to the production of bone at the periphery the area of bone destruction. Because organized osteoblastic activity is even slower than osteoclast activity, the ability of the host bone to "wall off" an osseous lesion implies that the lesional tissue must be expanding in a very slow manner. Lesions that give rise to this

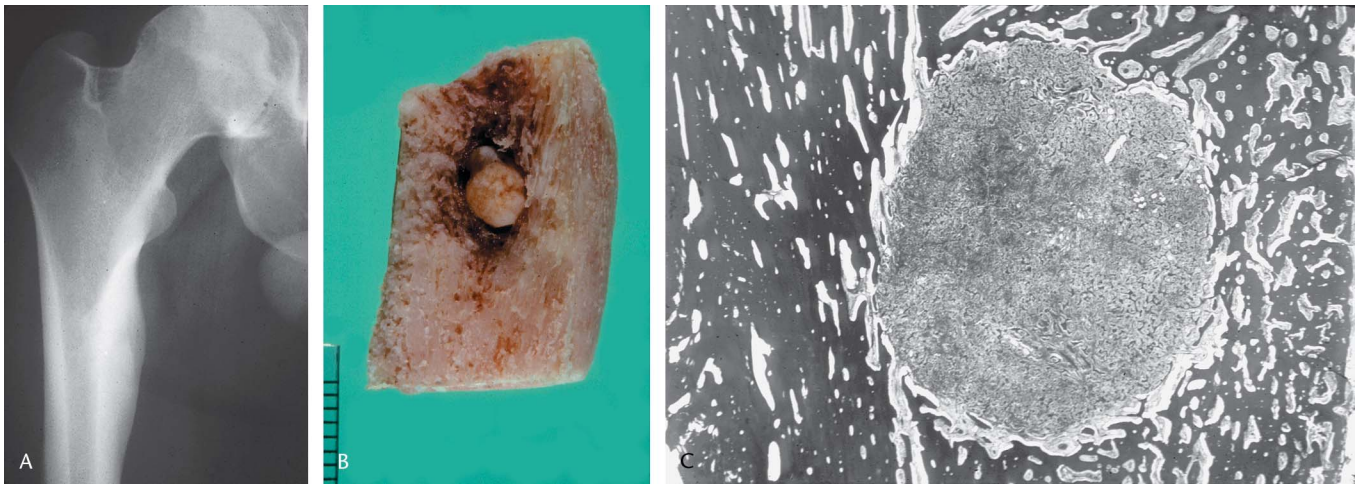

FIGURE 13. A, Osteoid osteoma with exuberant periosteal reaction. This 18-year-old had complained of exquisite pain waking him from sleep and relieved by aspirin. The dense, slowly developing continuous fusiform medial periosteal reaction has created so much new bone that the lesion can not be clearly seen on the radiograph. B, The midportion of the segment of thickened cortex was excised, revealing this 3- to 4-mm osteoid osteoma. It is easy to understand how this could be obscured by the surrounding remodeled cortex, which is 3 to 4 times thicker than normal. C, A low-power photomicrograph through the whole mount of the lesion demonstrates normal cortex with compact bone and normal Haversian systems on the left and portions of the less mature compact bone developing from the periosteum on the right.

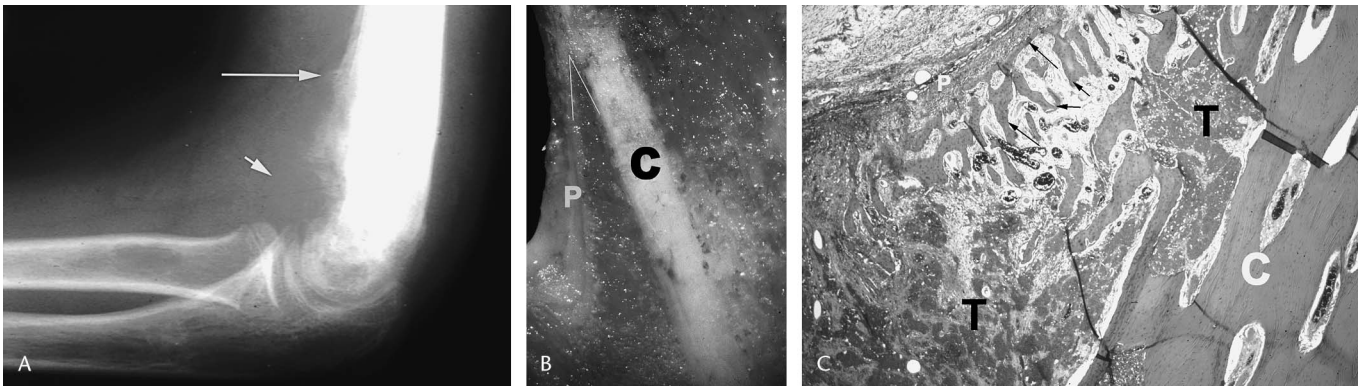

FIGURE 14. A, Codman angle associated with osteosarcoma. The arrow points to the area of periosteal reaction just before it joins the underlying cortical surface of the humerus proximally. The periosteal reaction at the distal end disappears as it approaches the soft tissue mass (short arrow). B, Gross appearance of a Codman angle. The cortex C and periosteum P are labeled and the angle where they join is outlined and can be compared with the radiograph. C, Codman angle, low power, demonstrates tumor T in soft tissue (lower left) and inside a Haversian canal (upper right). The periosteum (P) and its underlying new bone production crosses toward the cortex from upper left to middle center.

type of reaction are almost invariably benign, and sections made through the interface of lesional tissue and surrounding normal tissue usually demonstrate varying amounts of bone separating the two (Fig. 9A and 9B).

Lesions that are biologically more aggressive expand at a faster rate than the bone can be absorbed to accommodate them. As the lesion expands, it extends into the intertrabecular spaces of the bone not yet absorbed by osteoclasts first by displacing the fat stored within marrow adipocytes and extending along the inter-adipocytic septa. Following this, the tumor replaces the adipocytes and fills the intertrabecular spaces. In addition, lesional tissue may gain access to intracortical Haversian and Volkmann canals. If the lesion is neoplastic, it may grow in these vascular canals and extend to the subperiosteal space. If the lesion is an infection, it may also cause bone necrosis due to the secondary edema in the confined envelope of surrounding compacta. The process may then reach the vascular canals and subperiosteum by pressure. Because there are portions of the process that extend into bone and marrow for some distance further than the bone destruction, the transition zone in these places tends to be indistinct.

When portions of the transition zone are indistinct but other portions are somewhat defined, the resulting radiographic appearance has been termed "moth-eaten".[14] Histologic sections at the interface of these lesions and surrounding bone usually demonstrate permeation of adjacent marrow spaces

FIGURE 15. A, Onion skin periosteal type reaction shows several discontinuous layers of new bone formation outside the cortex (arrow). B, Histology of cortex and periosteal new reaction shows that the bone becomes thinner, less compact, and less complete going from inside (left) to outside (right).

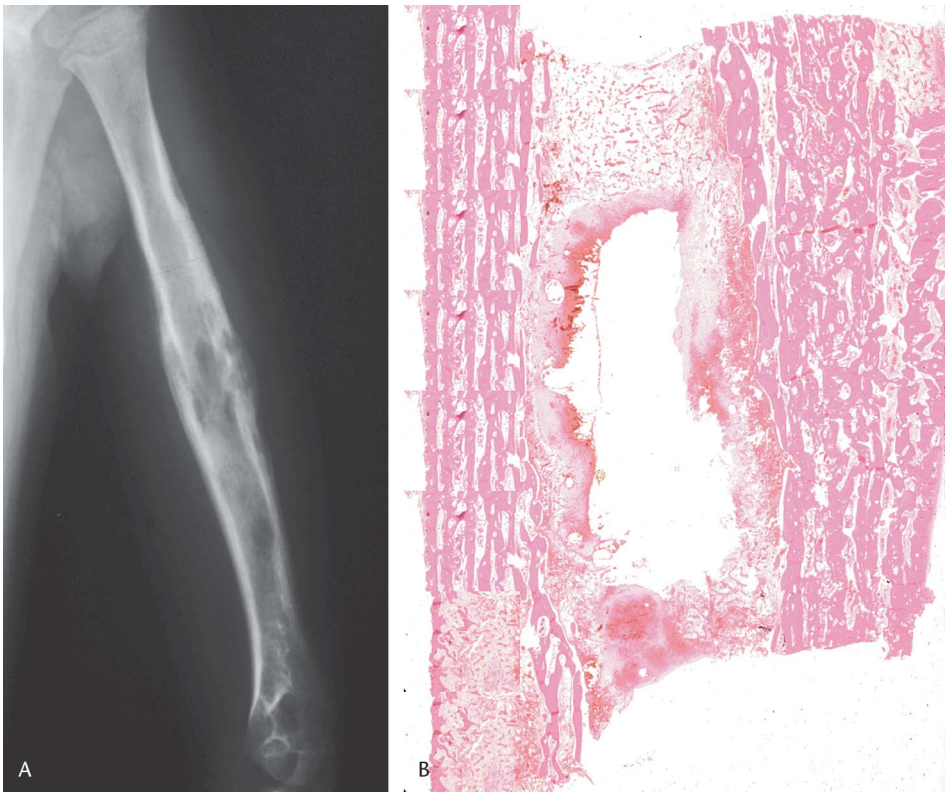

FIGURE 16. A, Oblique radiograph of patient with Ewing sarcoma treated with systemic chemotherapy. Note that the layers of periosteal reaction are fusiform and continuous whereas the underlying bone shows a moth-eaten pattern more typical of a slower-growing malignancy. B, Low-power whole mount of resected humeral shaft demonstrates many delicate layers of cortex with expanded Haversian systems. These layers are continuous and somewhat parallel. At the same time, there is no viable tumor left in the region.

that should normally contain fat or marrow. In the cortex, Haversian canals, which should contain vascular structures, may similarly show tumor or inflammatory infiltrates replacing them (Figs. 10A and 10B).

Processes that have the highest biologic aggressiveness have a radiographic appearance termed "permeative", which is usually associated with primary malignant bone tumors.[11] In this type of lesion, the tumor usually replaces the marrow for great distances without any significant osteoclastic reabsorption. Because the process replaces structures with fat radiodensity with those of water radiodensity but does very little to alter the bone structure, the radiographic findings may very subtle. On the other hand, a very large tumor volume is usually present, and despite the lack of bone destruction, it may be associated

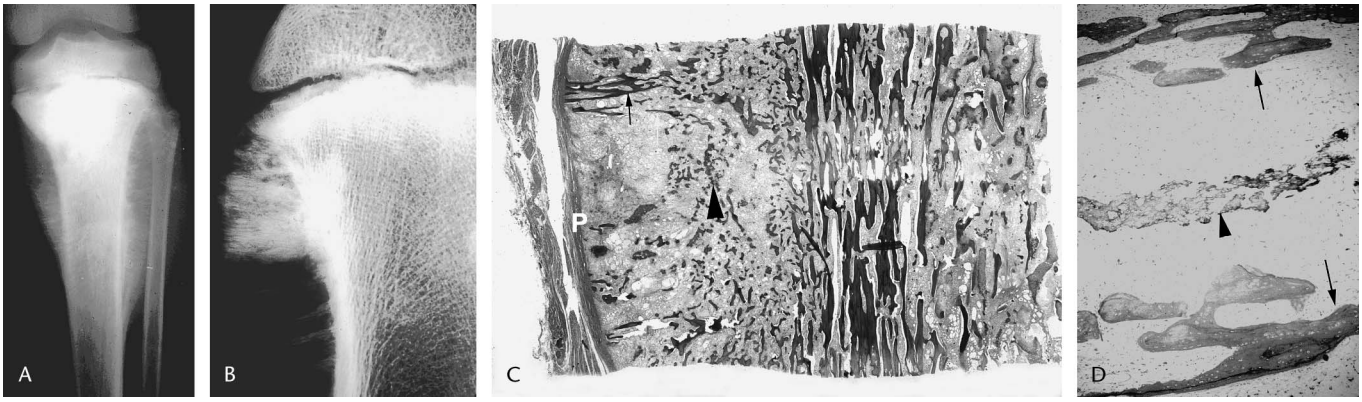

FIGURE 17. A, Osteosarcoma of the proximal tibia showing diffuse sclerosis and complex periosteal reaction with Codman triangles and so-called ''hair on end'' periosteal reaction. B, A specimen radiograph of one side clearly demonstrates vertically speculated new bone formation that is less dense at the periphery and more dense toward the cortex characteristic of reactive periosteal bone. At the same time, there is more fluffy and diffuse density between these spicules characteristic of tumor bone production. C, Low-power whole mount of periosteal reaction and underlying bone demonstrates elevated periosteum (P), periosteal new bone (arrow), and bone of tumor origin (arrowhead). The specimen has been removed following chemotherapy and there is little viable tumor remaining. D, Higher magnification of periosteal reaction demonstrates parallel streamers of periosteal new bone (arrows) and less regular tumor bone between them (arrowhead).

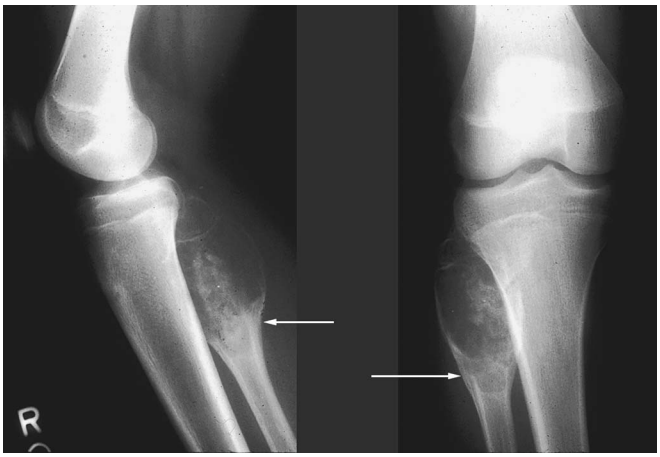

FIGURE 18. Aneurysmal bone cyst of the fibula in a 16-year-old male. The lesion is expansile (it is wider than the fibular growth plate) and the arrow points to a continuous, though multilayered buttress periosteal reaction. Note that the bony cortex above this reaction is intact but thin, indicating a rapidly expansile yet benign process.

with a large soft tissue mass. A biopsy of practically any area of a bone affected in this manner will demonstrate the process, even if the radiograph appears normal (Figs. 11A and 11B). It is only relatively late in the evolution of this process that radiographs demonstrate obvious destructive changes in the bone where the process is the oldest.

PERIOSTEAL REACTIONS

In addition to altering structure within a bone, lesions may also cause the periosteum to produce reactions that can be assessed radiographically. The periosteum consists of an outer fibrous layer and an inner pluripotential germinative layer, or cambium layer. Tough, collagenous strands, the Sharpey fibers, connect it to the cortex. These fibers are relatively lax in childhood and become shorter and more adherent to the cortex in adults. Although the periosteum is not usually seen in normal bone x-ray films, it may produce an osseous reaction if irritated. This reaction, in turn, is visible on roentgenographs.

The appearance of a periosteal reaction depends not only upon the nature of the process, but also upon the patient's age, because a more tightly attached periosteum is associated with a less exuberant reaction. Generally, indolent processes give rise to continuous or solid periosteal reactions. This is because it takes more time for osteoblasts in the periosteum to form an organized reaction than a disorganized reaction; indolent processes allow the periosteum this extra time.[12] A solid periosteal reaction often manifests as a thickened cortex, which may be linear or even fusiform radiographically depending upon the localization of the reaction (Fig. 12). Some benign lesions causing disproportionately slow periosteal irritation such as an osteoid osteoma or intracortical abscess may result in so profuse a production of periosteal new bone formation that the resulting radiodensity obscures the lesion itself (Figs. 13A–C).

Interrupted periosteal reactions usually indicate more rapidly evolving processes, such as hematomas, infections,

FIGURE 19. A, Interrupted multilayered (onion-skin) reaction from the fibular periosteum in Ewing sarcoma. There is a hazy soft tissue density surrounding the peri-fibular reaction. B, An angiographic study of the same patient reveals a very large tumor vascular blush corresponding to the hazy soft tissue reaction surrounding the fibula. The disproportionately large soft tissue mass with relatively little destruction of the underlying bone is typical of a highly malignant tumor.

and malignant tumors. Perhaps the best known of these is the Codman angle, characterized by a single layer of bone attached to the cortex at one end but extending discontinuously away from the cortex at the other end. The subperiosteal new bone is usually interrupted by the rapidly expanding soft tissue extension from the underlying osseous process, and the picture is one of an open radiodense angle without ossification at the open end (Figs. 14A–C). When an underlying malignant tumor is associated with a Codman angle, the cortex underlying the periosteal new bone may be indistinct or absent.

Interrupted periosteal reactions may be multilayered, or laminated, resulting from repeated sequences of periosteal elevation in small increments with successive layers of periosteal new bone being added after each sequence. They are often described as "onion skin" because of their successive layers.[16] Histologically, concentric strata of reactive bone are separated by loose, vascular connective tissue that may or may not contain a pathologic process. They are least mature and less continuous the further each stratum is away from the underlying cortex (Figs. 15A and 15B). Solid periosteal reactions may also have a multilayered arrangement, but each layer is continuous because less aggressive processes allow for the more complete maturation of each layer. It is notable that the successful institution of systemic chemotherapy for a bone tumor may slow down the process sufficiently to convert an interrupted multilayered periosteal reaction to a continuous multilayered periosteal reaction (Figs. 16A and 16B).

Complex periosteal reactions may also resemble sunbursts or hairs-on-end depending upon the manner in which they produce new bone. They often consist of an admixture of reactive bone and neoplastic bone matrix (Figs. 17A–D). The type of bone may often be discernible radiographically. Reactive bone tends to be zonal, producing a gradient of radiodensity, whereas bone produced by tumors is patternless.[3] Complex periosteal reactions are often indicative of an indolent process if continuous or an aggressive process if they are discontinuous.[7,12,16] A lesion with a buttress type of periosteal reaction in which many confluent layers are visible but that does not encase an entire lesion usually reflects a rapidly expanding lesion that still has a limited biologic potential (Fig. 18). Regardless of the type of periosteal reaction, any lesion thought to be a bone tumor radiographically should be considered malignant if there is a mass in the overlying soft tissue without obvious cortical disruption (Figs. 19A and 19B).

EXTRACELLULAR MATRIX

Whereas most of the alterations visible on skeletal radiographs are due to changes in the bone and reactions of the periosteum, they are also affected by the composition of the

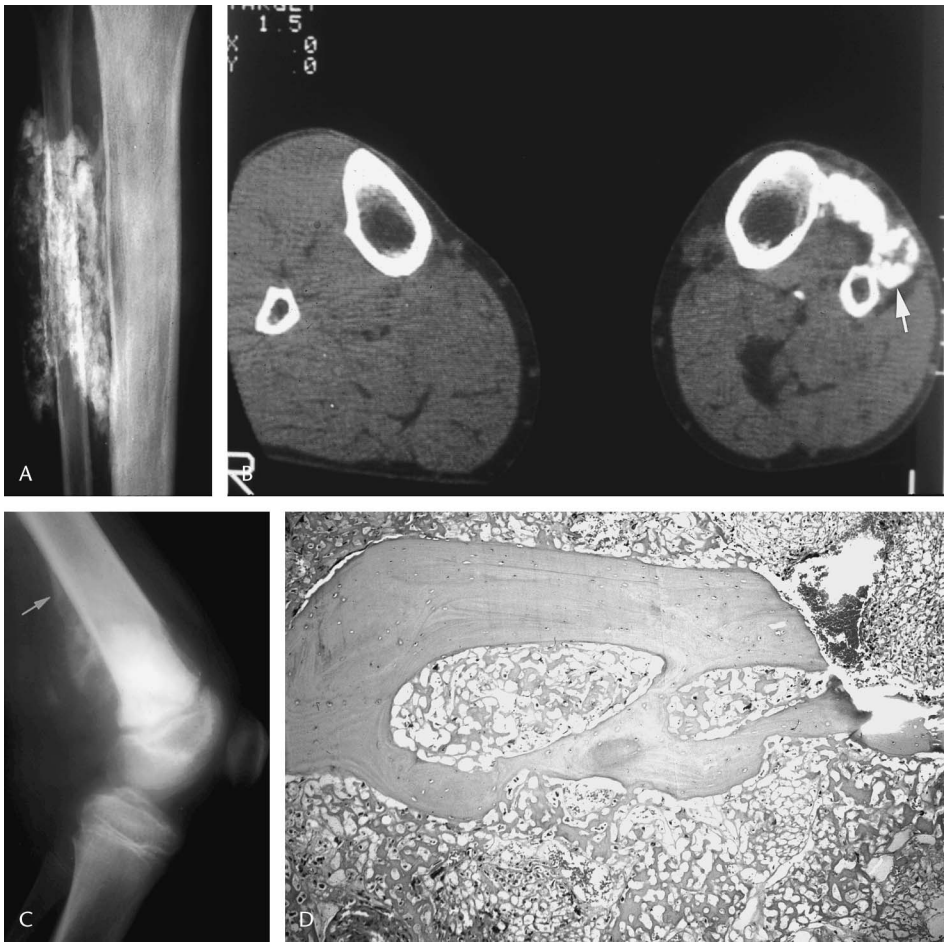

FIGURE 20. A, Reactive bone matrix in heterotopic ossification. The bone is arranged in what appears to be a peri-fibular location and is clearly trabeculated. B, CT scan of the same patient demonstrates that the ossification is entirely anterior to the left fibula and does not surround it. The arrow points to the dense outer portion of the lesion surrounding the more lucent center; this recapitulates the zonal phenomenon described in circumscribed heterotopic ossification. C, Osteosarcoma, lateral radiograph. Note that the distal femur is diffusely radiodense from the growth plate proximally; this cloudy or fluffy appearance is characteristic of mineralized tumor matrix. Some of the cloudiness extends into the posterior soft tissue mass distal to the Codman angle (arrow). D, A histologic section proximal to the growth plate of this femur demonstrates mature cancellous bone of the metaphysis surrounded by lacelike bone matrix produced by tumor cells and accounts for the increased radiodensity.

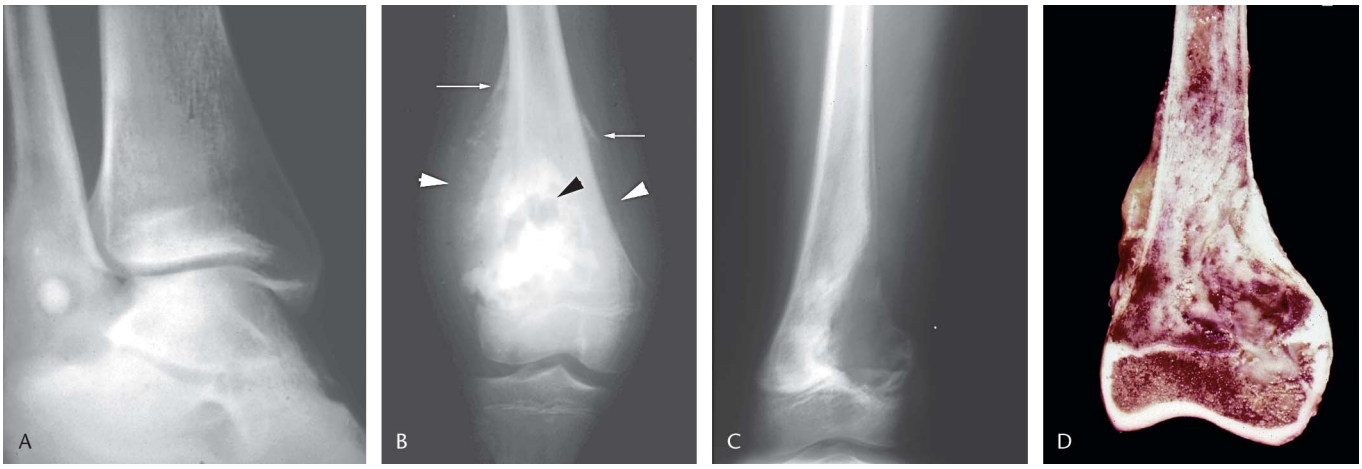

FIGURE 21. A, Osteoid osteoma, distal fibula. The routine oblique radiograph demonstrates a well-circumscribed radiolucency containing a well-circumscribed radiodensity appearing like a target. This is because the osteoid in the central portion of the lesion has mineralized to become bone and contrasts with the less mineralized matrix surrounding it. B, Osteosarcoma, distal femur. The irregular, poorly circumscribed, cloudy radiodensities are characteristic of tumor bone, and the proximal lateral and medial Codman angles (arrows) are indicative of tumor in the soft tissues (white arrowheads). Despite the radiolucency in the center of the lesion (black arrowhead), all areas of the specimen lesion appeared to have a uniform distribution of tumor bone histologically. Because the sections were all made following decalcification when bone could no longer be distinguished from osteoid, the area of lucency was probably due to areas of the tumor matrix that had not mineralized. C, Osteosarcoma, small cell type, distal femur. The radiograph demonstrates indistinct radiolucency extending focally past the growth plate and into the epiphysis. D, The specimen demonstrates a fair amount of bone destruction corresponding to these same areas. Histologically, there was very little osteoid matrix and many fields of viable cells corresponding to the radiolucent areas.

pathologic process itself. The production of extracellular matrix by skeletal tumors often gives rise to radiographic characteristics that indicate the dominant type of matrix produced.[8]

Bone matrix is radiodense, but the distribution of its radiodensity depends upon the manner of bone production. In general, the more mature and regular the bone formation, the more trabeculated it appears on a routine x-ray (Figs. 20A and 20B). Less organized bone formation, such as that seen in osteosarcomas, tends to look cloudy or fluffy, particularly if the bone formation is sheetlike histologically (Figs. 20C and 20D).

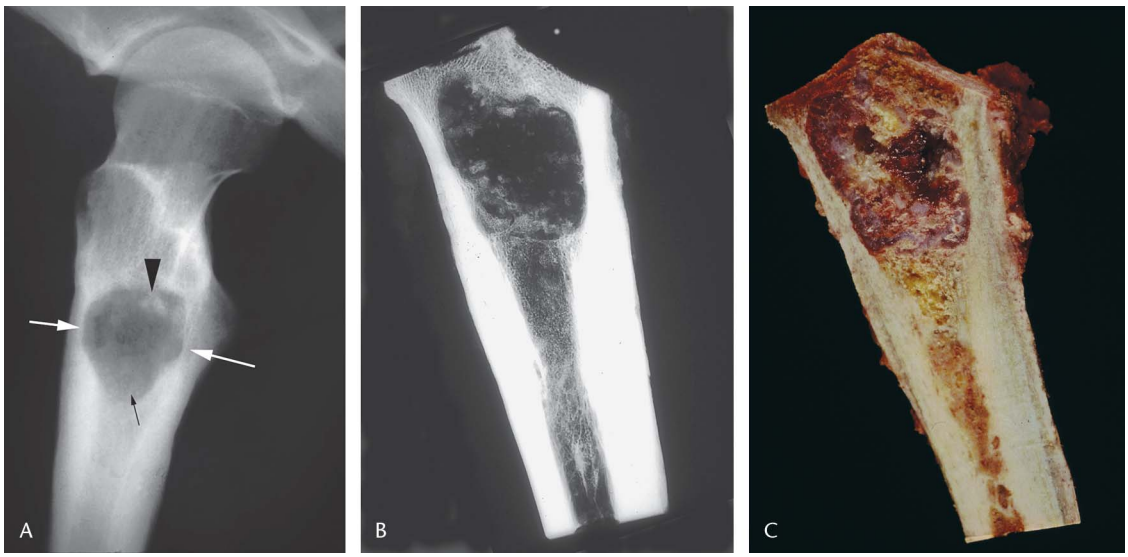

FIGURE 22. A, Chondrosarcoma, proximal femur, low-grade. The white arrows point to endosteal scalloping characteristic of lobulations of the tumor matrix. The black arrow points to subtle stippled matrix calcifications. The black arrowhead points to popcorn-like ossification. B, Specimen radiograph demonstrates peripheral scalloping, cortical thickening, and matrix calcifications and ossifications in better detail. C, Corresponding specimen reveals cortical endosteal scalloping and calcifying cartilage lobules of varying sizes.

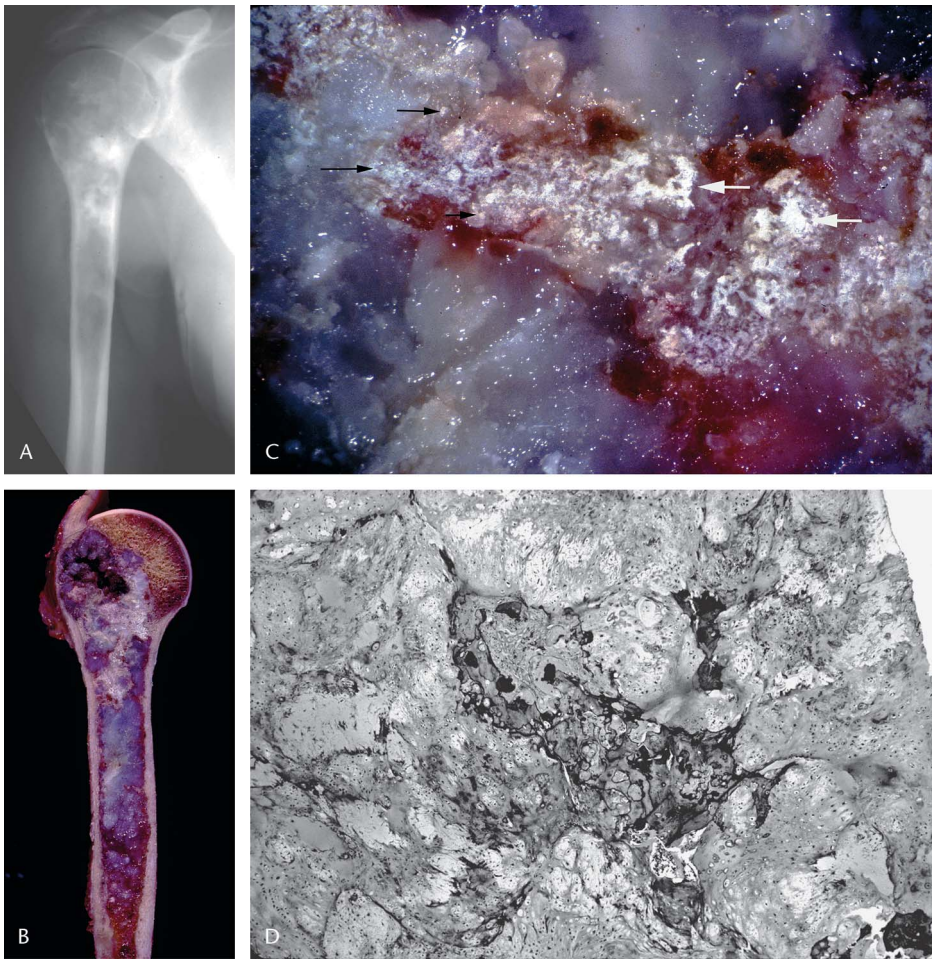

FIGURE 23. A,B, Clinical radiograph and corresponding specimen from grade 2 chondrosarcoma of the humerus. Note the popcorn ossification and ring-like ossifications proximally in the radiograph (A). The specimen (B) plainly illustrates that the popcorn areas of ossification contain whitish bone. Note also the lobularity of the cartilage matrix causing endosteal scalloping. C, Close-up gross photograph of cartilage matrix demonstrating lobularity of matrix, stippled calcifications (black arrows), and nodular ossifications corresponding to bone resembling popcorn on radiographs (white arrows). D, Histology of endochondral ossification in the center of a cartilage nodule. This corresponds radiographically to stippling but does not contain enough bone and is not sufficiently large to resemble popcorn radiographically.

Occasionally, an osteosarcoma with abundant immature bone formation is radiolucent. In this circumstance, it is worth noting that osteoid matrix is not mineralized; until it becomes mineralized osteoid has the same radiodensity as water. Because most histologic sections will have been completely decalcified prior to sectioning, the histologic section can not distinguish bone that has been decalcified from osteoid that has never mineralized. Clinical or specimen radiographs can help to make this distinction (Figs. 21A–D).

In the absence of calcification or ossification, cartilage matrix has the same radiodensity as water and is radiolucent. Cartilage matrix produced by tumors is almost exclusively

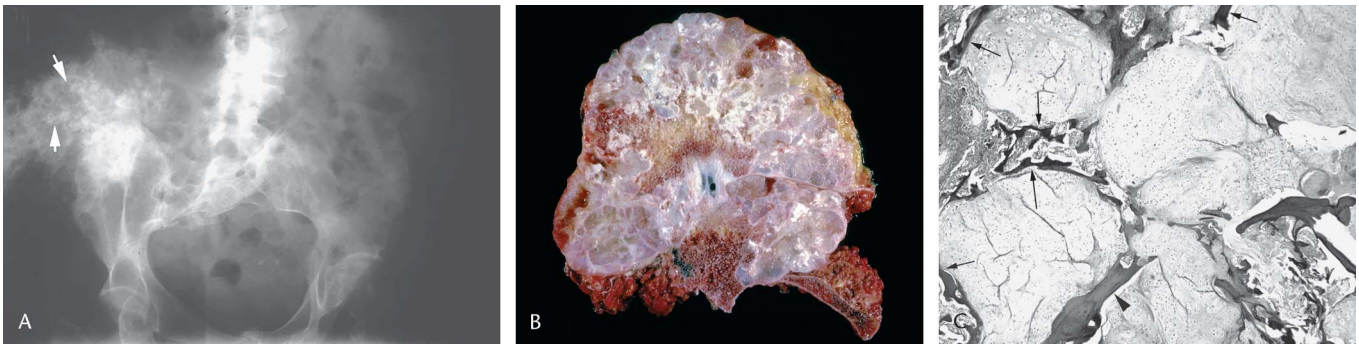

FIGURE 24. A, Chondrosarcoma of the left ilium arising from a previous solitary osteochondroma. This very large and bulky low-grade lesion demonstrates dispersed calcification, popcorn ossification, and confluent radiodense rings (arrows). B, Gross photograph of axial cut through specimen reveals multiple cartilage matrix nodules of varying size as well as stippled confluent calcifications with ringlike and nodular ossification. C, Photomicrograph demonstrates incomplete ringlike trabeculae of bone formed by endochondral ossification at the periphery of myxoid cartilage nodules (arrows). Arrowhead demonstrates pre-existent mature bone surrounded by permeating cartilage matrix.

hyaline in type. Like ordinary hyaline cartilage, neoplastic hyaline cartilage tends to grow clonally in spherical aggregates about groups of proliferating chondrocytes. Because these aggregates are largely water containing, a cartilage tumor in three dimensions has an arrangement and consistency resembling a bunch of grapes, except that the grapes themselves may vary in size from one grape to the next. This arrangement accounts for the lobularity of cartilage tumors; it is also why pressure scalloping of the endosteal cortex is often seen in routine x-rays of cartilage tumors (Figs. 22A–C; see also Fig. 7).

Ordinary hyaline cartilage is devoid of a blood supply; it can extract oxygen and nutrients by diffusion into its watery matrix for a distance of 1 to 2 cm from the nearest blood vessels. Neoplastic hyaline cartilage also has no blood supply. As its lobules increase in size, its capacity to nourish itself by diffusion diminishes. Local conditions, including ischemia and pH changes, result in matrix calcifications that may be seen as radiodense stippling on x-ray films. Calcification of the matrix further impedes cartilage nourishment and respiration and the cartilage may undergo necrosis. This is usually associated with secondary neovascularization and replacement of the cartilage by bone, or endochondral ossification.[17] Should this ossification occur in the center of cartilage nodules, it appears radiographically as trabeculated nodules that resemble popcorn (Figs. 23A–C). Often, this type of ossification occurs at the periphery of the cartilage nodules, where it may form radiodense shells of varying completeness about these nodules. Incomplete shells are seen as trabeculated curvilinear radiodensities, whereas more complete shells appear as radiodense rings, which are easily identifiable histologically (Figs. 24A–D).[8] This type of ossification should be distinguished radiographically and histologically from the bone of neoplastic origin occurring in osseous tumors because the prognosis is better in most tumors of cartilaginous origin.

Fibrous tissue, like other types of soft tissue, is radiolucent. When fibrous matrix is present in bone, it must either occupy a significant amount of cancellous bone volume to be appreciable radiographically or it must be in a cortical location where it can be seen with an appropriate view.

The most common space occupying fibrous lesion of bone is fibrous cortical defect/nonossifying fibroma. This lesion is characteristically radiolucent, eccentric, metaphyseal, and has a sclerotic, scalloped border. Its long axis is almost always parallel to the shaft of the bone. Because it is almost always cortically based and has a sclerotic border, it is usually easily visible in either of the two routine radiographs taken at right angles (Fig. 25A). It affects 25% or more of individuals and it is so unique radiographically that a diagnosis can be ascertained with greater than 99% certainty on routine x-rays.[18] Its histology demonstrates a fibrohistiocytic lesion containing spindle cells, multinucleated giant cells, and occasional foamy histiocytes (Fig. 25B). These cells are often arranged in a prominent storiform pattern. Sometimes, noticeable mitotic activity

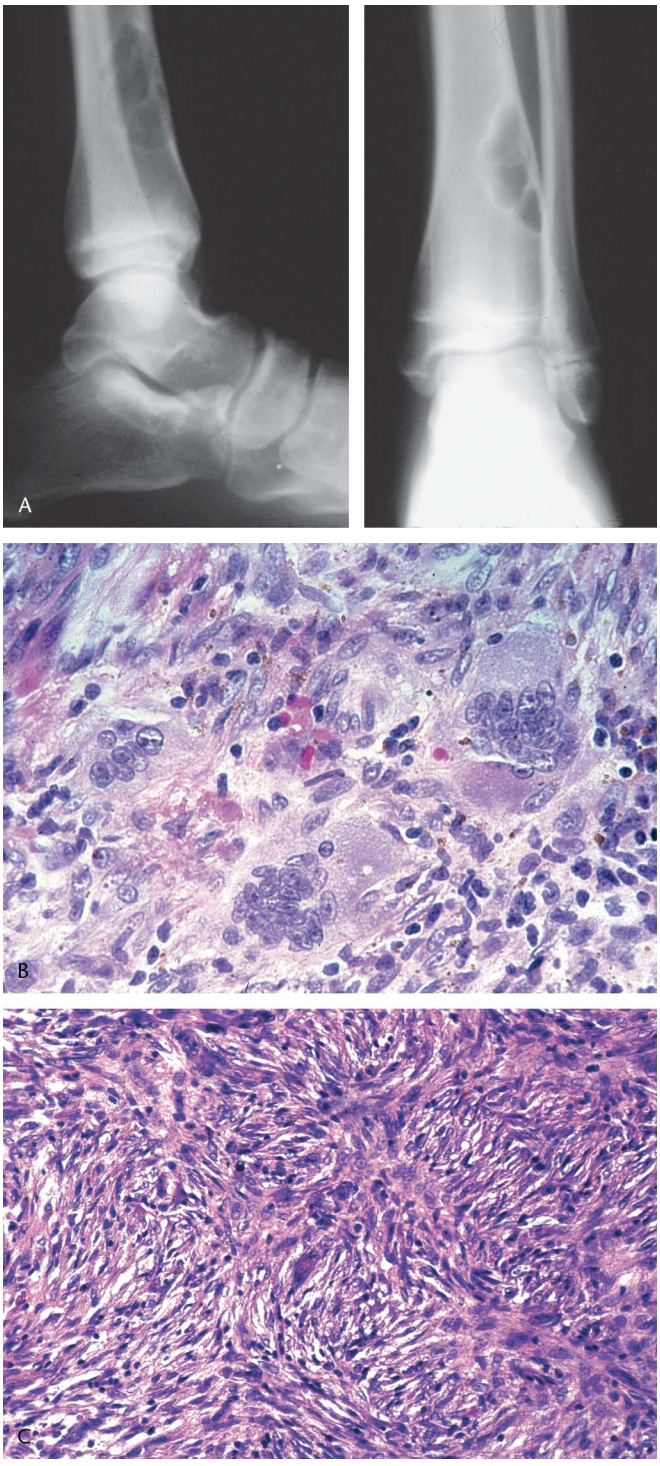

FIGURE 25. A, Nonossifying fibroma. Lateral and anteroposterior views demonstrate an elliptical radiolucent defect in the lateral distal tibial metadiaphysis. The lesion is eccentric, cortically based, and has scalloped, sclerotic borders. B, Nonossifying fibroma. High- power field reveals fibrohistiocytic nature of the lesion with multinucleated giant cells, mononuclear histiocytes, and fibroblasts. Note the presence of hemosiderin pigment. C, Nonossifying fibroma. The typical histology of this lesion demonstrates the rather cellular and storiform pattern characteristic of most areas of this lesion. Such areas should not be interpreted out of context with the radiographs.

FIGURE 26. A, Fibrous dysplasia. Radiograph of the elbow demonstrates two lesions, one in the humerus and the other in the proximal radius. The humeral lesion has a lightly cloudy appearance like ground glass proximally and is more radiolucent distally. This may be because there is more cortical attenuation distally or because the distal portion of the lesion has undergone encystification. Note that the humerus shows an increase in diameter and that the distal margins of the lesion and bone interface appear sharp. B, Fibrous dysplasia. The lesion occupies the entire femur, which is coarse and expanded. There is a bowing (varus) deformity of the diaphysis and a varus deformity of the widened femoral neck. This typical radiographic appearance is called a ''shepherd's crook'' deformity. There is also a lesion in the ischium and in the pubis; fibrous dysplasia often involves multiple bones in a single limb-bud distribution (monomelic, polyostotic fibrous dysplasia). C, Fibrous dysplasia, interface of lesion with cortex shows cortical thinning with expansion of Haversian systems and increased porosity of compact bone (right). Note the formation of bone microtrabeculae in the fibrous stroma.

or hyperchromatic nuclei are present (Fig. 25C). Occasionally, a nondisplaced microfracture adds immature bone or osteoid to the picture. Consequently, if the characteristic radiographic appearance of the lesion is not communicated to the pathologist and the radiograph is not correlated with biopsy material, it may be tempting histologically to make the diagnosis of benign or malignant fibrous histiocytoma, giant cell tumor, and even osteosarcoma.

The next most common space occupying fibrous lesion of bone is fibrous dysplasia. Like fibrous cortical defect, fibrous dysplasia is usually well delimited. Unlike fibrous cortical defect, it is situated in the medullary cavity, and it only

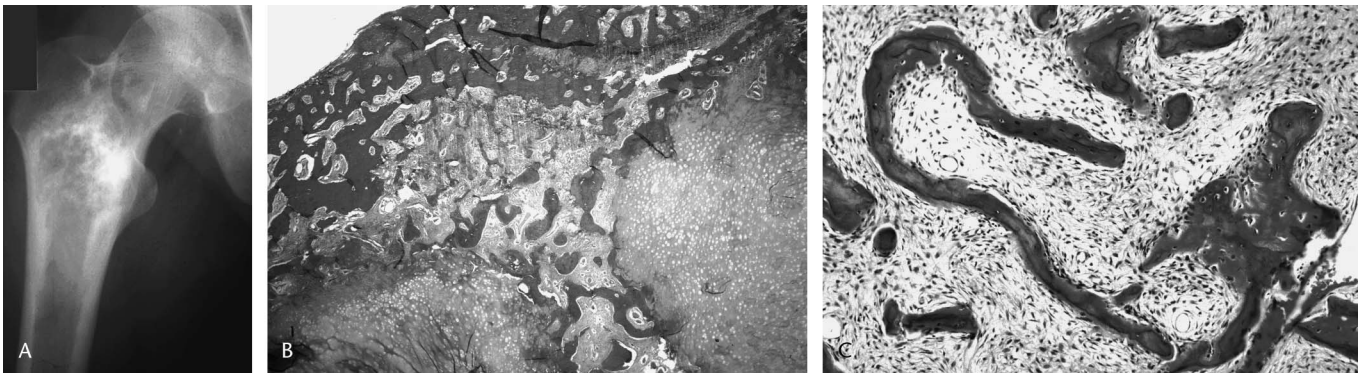

FIGURE 27. A, Fibrous dysplasia producing exuberant cartilage. This lesion in a middle-aged male was thought to be a cartilage tumor because of its popcorn and incomplete ringlike calcifications in this somewhat lucent lesion of the trochanteric region of the femur. B, Low-power histology demonstrates expansile cartilage nodules partially surrounded by bone in ringlike fashion. There is some fibrous tissue producing bone microtrabeculae (center) and the overlying cortex is intact. C, Areas of the fibrous tissue away from the cartilage matrix producing the immature curved bone spicules typical of fibrous dysplasia.

rarely produces a defect in the cortex. On the other hand, it is often expansile, and may cause cortical thinning by pressure. In addition, its fibrous stroma usually contains numerous well-distributed microtrabeculae of woven bone. This fibrous stroma is more radiodense than the usual fat of the marrow cavity, and its mineralized bone trabeculae impart a hazy, vaguely radiodense appearance to the lesion that has been characterized as a "ground glass" appearance.[12] This combination of findings is highly suggestive of fibrous dysplasia although it is not as statistically certain an x-ray diagnosis as fibrous cortical defect/nonossifying fibroma. Sometimes, the diameter of the bone is increased in fibrous dysplasia. There may also be modeling deformities and other deformities secondary to the slow effects of gravity on weakened bone (Figs. 26A–C).

Because fibrous dysplasia can recapitulate any histologic combination of bone development, it sometimes contains cartilage in addition to immature bone. When its cartilaginous component is dominant, fibrous dysplasia resembles cartilage tumors radiographically and the lesion is sometimes referred to as fibrocartilaginous dysplasia.[2] In this instance, it is the pathologist who must find histologic evidence of usual fibrous dysplasia to make the correct diagnosis (Figs. 27A–C). Rarely, biopsies from lesions that are characteristic for fibrous dysplasia radiologically may demonstrate no bone formation at all.

By correlating imaging studies with histology, two other lesions with a low-grade malignant potential can be distinguished from fibrous dysplasia even though they are histologically similar. Low-grade central osteosarcoma usually has a radiologic appearance suggesting a more aggressive lesion than its histology (Figs. 28A–C). Parosteal osteosarcoma of the usual low-grade variety may have an identically indolent histology, but its radiographic appearance is that of a variably radiodense lesion usually attached to the surface of a long bone (Figs. 29A–D).

COMPLEMENTARY IMAGING STUDIES

There have been many advances made in imaging techniques, including radioisotopic bone scanning, plane tomography, computerized tomography, magnetic resonance imaging, and positron emission tomography. However, the production and interpretation of satisfactory routine radiographs is by far the most important imaging in skeletal disease. Whereas each new imaging technique has added to our diagnostic armamentarium, any given study, regardless of its increased sensitivity, is merely complementary to the routine x-ray studies. Consequently, specialized imaging studies should not be sought in place of plain roentgenographs. In fact, any special imaging study should only be ordered when routine radiographs or a less expensive or a less invasive imaging technique cannot answer a diagnostically important question about a given lesion (see Table 1).

Bone Scintigraphy

Radioisotopic bone scanning, or bone scintigraphy, uses radioactive tracer substances that have a short half-life and a high affinity for osteoblastic activity (eg, Technetium^{99}).

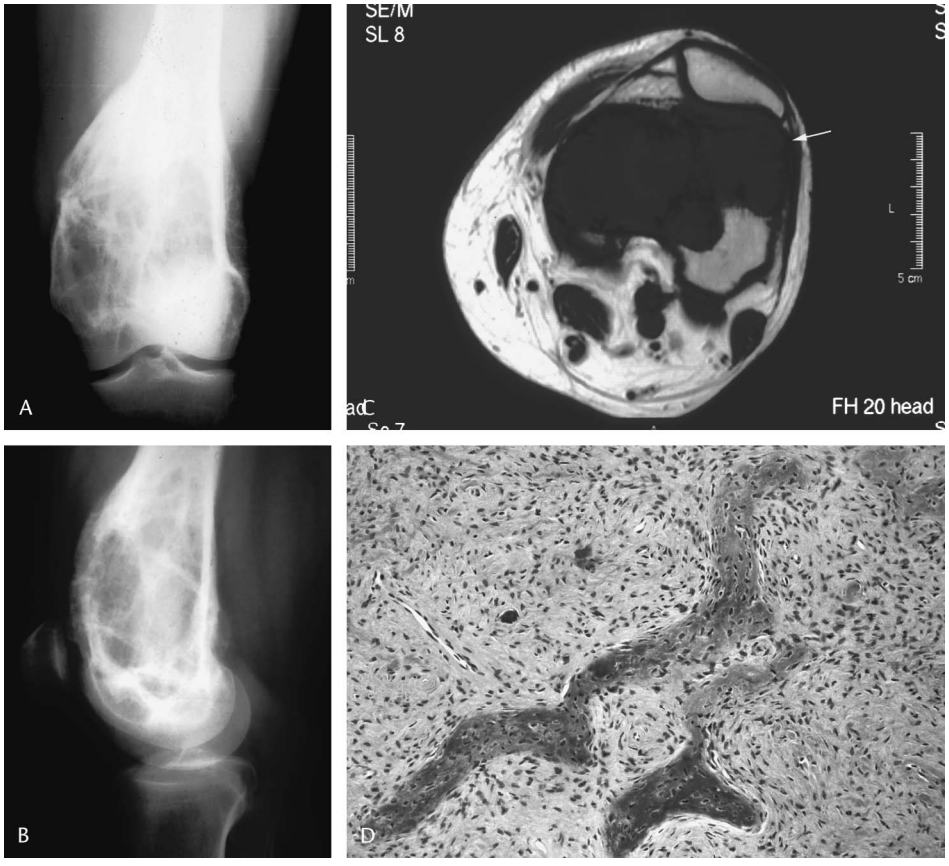

FIGURE 28. A, Low-grade central osteosarcoma. AP view demonstrates an expansile, trabeculated distal femur. There is a slightly radiodense lateral periosteal reaction. B, Low-grade central osteosarcoma. Lateral view demonstrates a small posterior soft tissue mass. C, Low-grade central osteosarcoma. A T_1 weighted axial MRI confirms the extraosseous extension of the lesion (arrow) and strongly favors a malignant neoplasm. D, Low-grade central osteosarcoma. A high-power photomicrograph demonstrates microtrabeculae of woven bone arising in a fibrous stroma virtually indistinguishable histologically from fibrous dysplasia. There is not enough atypia to suggest malignancy histologically, but the diagnosis is strongly favored by the imaging studies.

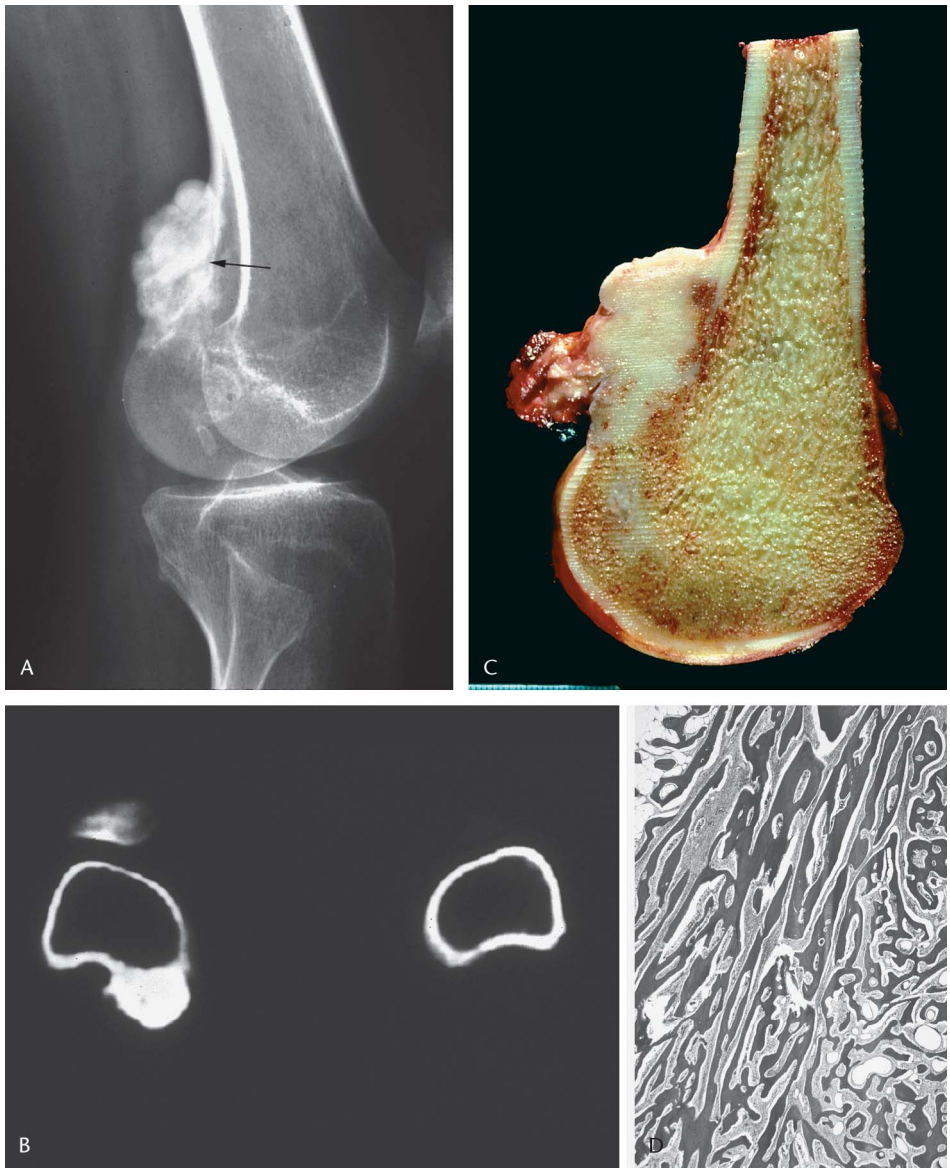

FIGURE 29. A, Parosteal osteosarcoma. Oblique radiograph of the distal femur demonstrates a radiodense lesion on the posterior surface of the femur containing some radiolucencies and appearing somewhat less dense at its periphery. Note that there is no periosteal new bone, and in fact, there is a subtle radiolucent line between parts of the mass and the underlying cortex. This line (arrow) represents the periosteum interposed between the expanding lesion and the underlying cortex. B, CT scan confirms the radiodensity of this lesion and its adherence to the cortex. There is neither medullary invasion nor periosteal reaction. C, Gross specimen demonstrating that the mass arises from the posterior surface of the distal femur and is intimately connected with its cortex. D, Parosteal osteosarcoma, low grade. A low-power photograph demonstrates trabeculae of bone that seem oriented in the same direction but show no real gradient of maturation. Note that the intertrabecular spaces are filled with fibrous tissue rather than fat. The collagen of these trabeculae is woven rather than lamellar. The combination of fibrous tissue and woven bone organized into microtrabeculae could be taken histologically for fibrous dysplasia were it not for the radiograph. It is, however, unusual for fibrous dysplasia to show any degree of trabecular orientation.

Consequently, it reflects physiologic events more than anatomic events.[19] Scintigraphy is particularly useful in assessing early alterations in bone metabolism as a result of local events. This is because cellular activity takes place very quickly but the resulting alterations in bone structure take place very slowly. For instance, bone scanning may detect local osseous reaction to a focus of infection or avascular necrosis within a day of the onset of the process. Bone scanning is also a useful way to detect diffuse metabolic diseases like hyperparathyroidism or widespread bone metastases long before these processes are detectable on a skeletal x-ray series (Figs. 30A–D). Conversely, certain lesions that cause bone destruction but have no surrounding reactive sclerosis (eg, multiple myeloma) may demonstrate obvious radiolucencies on routine radiographs but show no uptake on scintigraphs.

Plane Tomography

Plane tomography is a radiographic technique in which the x-ray tube and the cassette (or detectors) move in opposite directions to one another with respect to the patient. The area closest to the pivot point between source and cassette moves the least and stands out in contrast to the remaining structures, which are blurred. By moving the apparatus closer or further from the object of study, serial slices in which the areas of interest are in relative focus are prepared.[5,6] This technique is useful in evaluating overlapping details in bone such as fracture lines or edges of tumors, and has been used to discriminate between osteosarcoma and exuberant reactive bone in nondisplaced fractures[20] but it is expensive and has been largely replaced by computerized tomography (Figs. 31A–C).

TABLE 1. Summarized Attributes of Imaging Studies

Imaging Technique	Principle	Chief Advantage	Disadvantages	Usual Appearance
Routine X-rays	X-rays directly used to generate a two dimensional image of bone and soft tissue.	Provides the entire anatomic picture of the region of interest. Should be the screening procedure for all other imaging studies.	Relatively insensitive. Requires multiple views.	Air-Black Fat-Dark grey Other soft tissues- Lighter grey Bone, calcium, heavy metals- White
Plane Tomography	Same as in routine X-ray except that the X-ray source and detector are moved relative to a stationary patient. The pivot point between source and detector appears most focused; the remainder is blurred.	Provides the entire anatomic picture, but increases the sensitivity of routine X-rays by isolating specimen planes.	Expensive and becoming less generally available.	Same as routine X-rays.
CT Scanning	A computer measures the difference between incident and absorbed X-rays in a slice of tissue of designated thickness. The image is a map of tissue density in the slice.	Increases the sensitivity of X-rays by isolating thin tissue slices. Very good resolution permits fine analysis of compact bone changes. Can be used to measure tissue density precisely.	Poor contrast. Soft tissues are not well visualized. Because lesional areas may be small, tissue slices may not incorporate pathology.	Same as routine X-rays, but sensitivity increased.
MRI	Nuclei are polarized by a magnetic field. A radiofrequency signal deflects their dipole moments from the magnetic field and during the deflection causes them to give off the same radiofrequency signal. This signal is examined by a radiofrequency detector and plotted with respect to time.	Very high inherent contrast demonstrates details in soft tissues not revealed by CT scan.Can distinguish between fat, muscle, fibrous tissue. Shows circulatory alterations and edema as well as the ability to delimit the true boundaries of tumor and normal tissue.	Poor resolution. Bone generates no detectable signal. Tissue slices may not incorporate pathology for same reasons as in CT.	T_1 Weighting / T_s Weighting Fat: Very bright / Bright Water: Dark (Hypointense) / Bright (Hyperintense) Fibrous Tissue: Dark / Usually Dark Bone: Very dark (Signal void) / Very dark (Signal void)
Bone Scintigraphy	A radioisotope with a short half-life that localizles to areas of bone formation is injected intravenously. A gamma counter is passed over the body and localizes areas of uptake.	Demonstrates physiologic changes when there is early reactive bone long before anatomic changes can be detected by X-ray or CT scanning. Examines the entire skeleton at once.	Lesions that are not bordered by reactive bone may show no uptake even if the changes are visible on X-rays.	Bone forming reactions demonstrate high uptake (brightness).

Computerized Tomography

Computerized tomography is an x-ray–based technique in which a variable number of x-ray sources are coupled to their own x-ray detectors via computer. The computer calculates the difference between energy leaving the source and that reaching the detector and plots the difference in a two-dimensional map via Fourier transform. The image is essentially a map of radiodensity, and in fact the radiodensity can be measured with exquisite sensitivity by this technique.[9,21] Penetration may be windowed for tissues of different densities by manipulating the computer software.[23] The resulting images are identical to what would be obtained by slicing the body part into thin parallel sections ranging from a millimeter to a centimeter or more in thickness, and making contact specimen x-rays of each slice.[21] In other words, objects can be examined with surgical sensitivity without performing surgery. CT is capable of detecting very small differences in tissue density. It has very good resolution, so it is useful in detecting small abnormalities in bone. Because it detects lesions in bone with greater sensitivity than conventional x-rays, it is very useful in defining the extent of lesions in cancellous bone that destroy less than 40% of the cancellous bone volume (Figs. 32A and 32B). On the other hand, it has poor contrast, and it is not as good as MRI for evaluating differences in soft tissue.[24] It should also be remembered that CT is only sensitive when it is used correctly. Small lesions may be missed if the CT slices are too thick. If the slices do not incorporate the portion of the bone containing a lesion (this is the reason for doing scout x-rays prior to CT), the correct portion of the bone may be left out of the study.

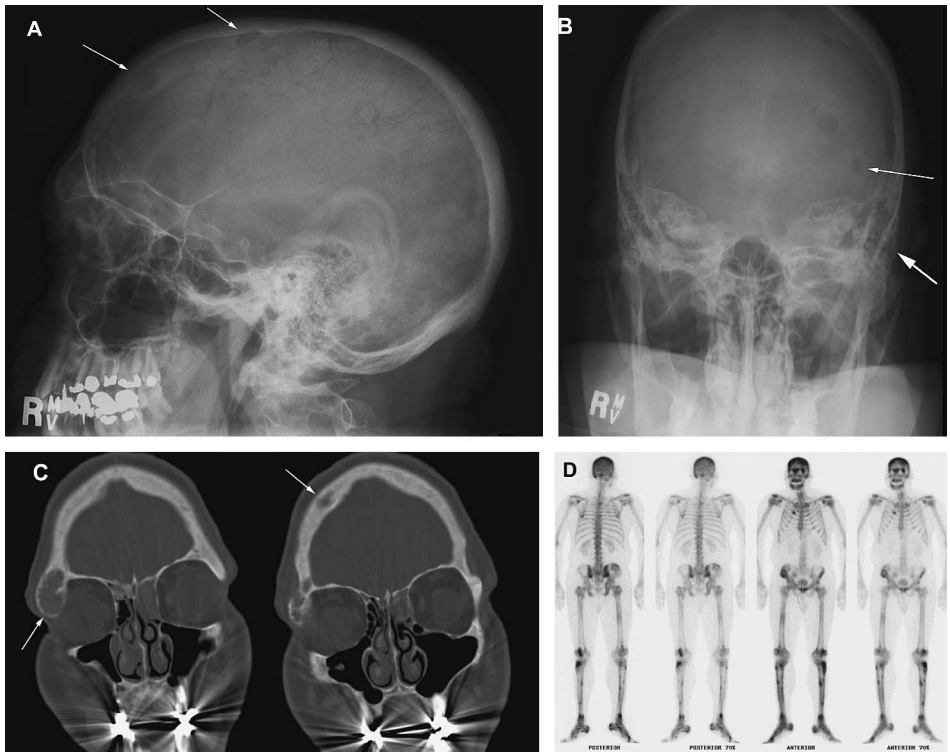

FIGURE 30. A–D, A 47-year-old man with asymptomatic hyperparathyroidism presented with slight unilateral proptosis. Lateral (A) and AP (B) skull films revealed multiple radiolucent lesions of the calvarium (thin arrows) as well as a left supraorbital space-occupying mass lesion (fatter arrow, B). Coronal CT (C) views better demonstrated the supraorbital mass, but also confirm other lucent lesions (arrows). Note also, that the normal skull tables and diploe are indistinct. The radiographic diagnosis of myeloma was suggested, but serum protein electrophoresis was negative. A technetium bone scan (D) demonstrates multiple areas of increased uptake not only in the skull but in both legs and in one rib. The combination of lytic lesions and increased uptake on bone scan is more typical of metastatic carcinoma than myeloma; however, the presence of metastases in both legs and in the skull without significant axial or proximal bone involvement would be very unusual. A biopsy of the orbital lesion revealed fibrous tissue, hemosiderin, multinucleated giant cells, and increased osteoclastic activity of the overlying cortex. It was suggested that the entire presentation might be due to hyperparathyroidism despite three normal serum calcium levels. An assay for intact parathormone revealed levels 50 times above normal baseline. The patient subsequently had a 2.5 g parathyroid adenoma removed.

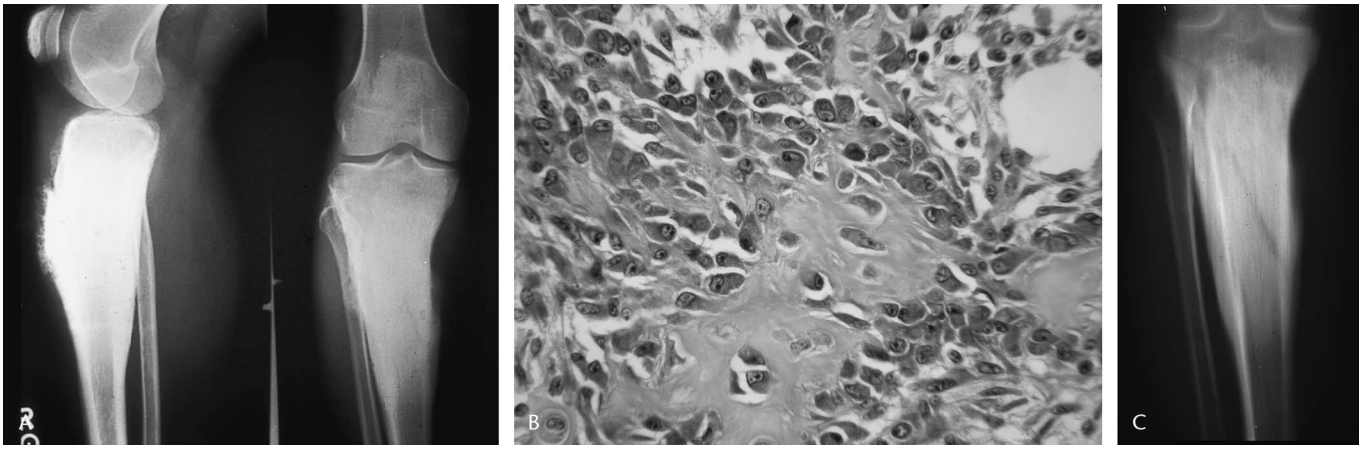

FIGURE 31. A, A 47-year-old man presented with painless swelling of the right lower extremity. Lateral and AP radiographs demonstrated osteosclerosis of the proximal tibia with a hair-on-end periosteal reaction. B, A biopsy of the soft tissue demonstrated fibrous tissue with differentiated osteoblasts lining the trabeculae. Elsewhere, there was cartilage and bone admixed, but always with an appositional osteoblast pattern. Although the osteoblasts are quite prominent, there is no discernible mitotic activity or pleomorphism. A suggestion was made that the biopsy represented fracture callus or reactive bone. C, A plane tomograph of the right lower extremity clearly demonstrates a diagonal fracture line through the sclerotic lesion. Sclerosing osteosarcomas usually do not fracture. Moreover, they are highly unusual in individuals in the fifth decade. Subsequently, it was revealed that this patient had practically no pain sensation secondary to chronic alcoholism. In addition, he had no proprioceptive sense because of tabes dorsalis. This combination of diseases enabled him to easily sustain a nondisplaced impacted fracture and walk on it without pain, causing an exuberant callus.

FIGURE 32. A, A conventional radiograph of a knee in a 16-year-old female with severe joint pain reveals a normal joint space but suggests a well-circumscribed, lucent lesion in the medial portion of the distal lateral femoral condyle. B, A CT scan taken axially through this area demonstrates a lucent lesion with an anterior area of sclerosis very clearly. Notice that the total amount of bone destroyed from anterior to posterior is no more than 50% to 55%; however, in this projection, the patella partially overlaps most of the lesion and so to the x-ray beam less than 40% of the bone is destroyed. If the x-ray film were seen in the lateral projection, only 25% of the bone would be destroyed and the lesion would remain invisible. This demonstrates the increased sensitivity of CT scanning over conventional radiography—provided that the CT scan actually cuts through the lesion! Note also, that the CT demonstrates a small amount of mineralized content in this lesion, which is a chondroblastoma and does contain small amount of mineralized chondroid matrix. About 33% of chondroblastomas have demonstrable mineral on conventional x-rays. This increases to about 50% on CT scans.

Magnetic Resonance Imaging

Magnetic resonance imaging (MRI) is a technique using the radiofrequency portion of the electromagnetic spectrum rather than its x-ray portion. In a magnetic resonance imager, a patient is placed inside a very strong magnetic field, which causes alignment of the dipole moments along the axis of the magnetic field lines. A pulse of radiofrequency is then given to the patient at the Larmor frequency.[22] This frequency is the arbitrary number of cycles per second to make protons resonate at any given magnetic field strength; it is directly proportional to the strength of that magnetic field.

The radiofrequency signal externally applied to the patient increases the kinetic energy of protons and neutrons; it causes a deflection of their dipole moments out of alignment

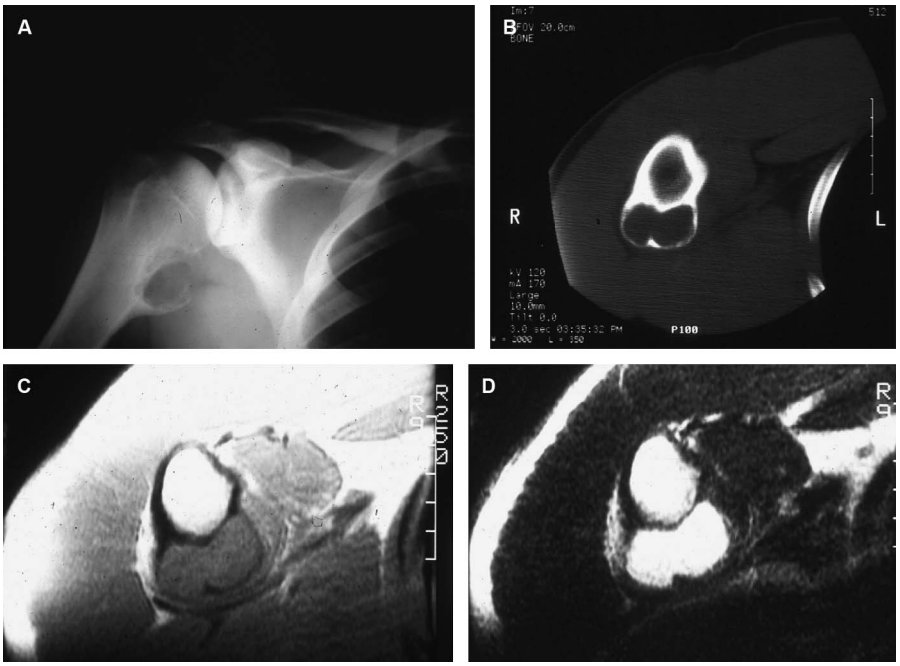

FIGURE 33. A–D, Lesion of proximal right humeral surface in a 28-year-old man seen by conventional x-ray (A), CT scan (B), MRI (C,D). The routine radiograph demonstrates a lesion on the medial surface of the cortex; the interior of the bone is somewhat scalloped, and there is a thick shell covering the lucency inferiorly. The entire picture looks like a volcano crater turned sideways. The CT adds to the information by demonstrating that the shell of bone outside though delicate and thin is complete and that the underlying cortex is pressure eroded but not violated. Figure C is a T_1 weighted MRI. Notice that the bright signal comes from the subcutaneous fat and the marrow (fat gives a bright signal, or is hyperintense, on T_1 weighted images). The lesional contents, which are about as dark as the surrounding muscle and less dark than the bone, are different than those of the fat. Figure D is a T_2 weighted MRI. Whereas the fat appears much the same, the lesion is now hyperintense. Fluid, or water-containing lesions are bright on T_2, so this lesion contains a fair amount of water. Histologically, the lesion was cartilaginous, and because of its location, size, and lack of destructiveness demonstrated on these studies, was called periosteal chondroma.

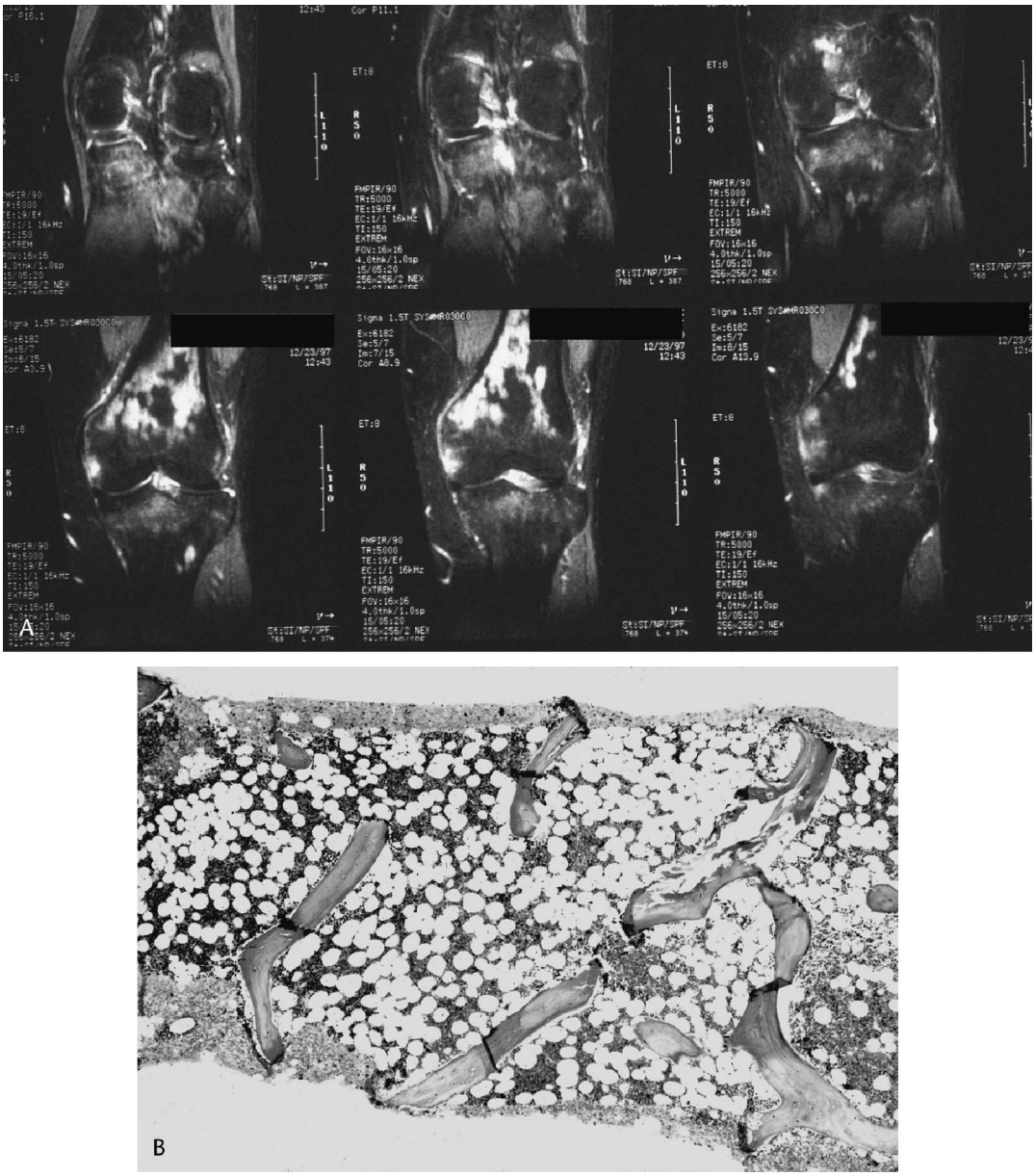

FIGURE 34. A, A 44-year-old woman had vague knee pain. Conventional radiographs were normal, and an MRI was performed (A). The study shown here is a fat- suppressed image. Areas of normal fatty marrow are hypointense, or black. The hyperintense areas, which are not pure fat, stand out as bright. A biopsy of one of the bright areas revealed normocellular hematopoietic marrow (B). All of the bright areas were thought to represent hematopoietic marrow that for some unknown reason had expanded more distally in the femur that would normally be seen at this age. The hematopoietic marrow was responsible for the bright signal that was not in itself abnormal but unusual for site. One of the dilemmas about MRI is that its contrast and sensitivity sometimes imparts more information than is diagnostically necessary or desirable.

with the magnetic field lines.[23] Without additional radiofrequency signal pulses, the resonance energy is lost over time, the dipole moments tend to return to the direction of the magnetic field lines, and the signal strength decays. This radio signal and its rate of decay are measured by a signal detector and plotted in three dimensions by Fourier transform.[21] The observed signals are generated with radiofrequency pulse sequences designed to make specific tissues respond with arbitrarily defined losses in radiofrequency energy.

Images generated by this technique appear as sequential slices and thus resemble those generated by CT, particularly when they are made in an axial plane. Although resonance can be induced in the atoms of many elements, signal detection is dependent upon an element having an odd number of nuclear particles. This is because half of the dipole moments of nuclear particles point in opposite directions, so that in elements with even numbers of particles, the wave fronts produced by resonance are exactly superimposed and cancel each other out.

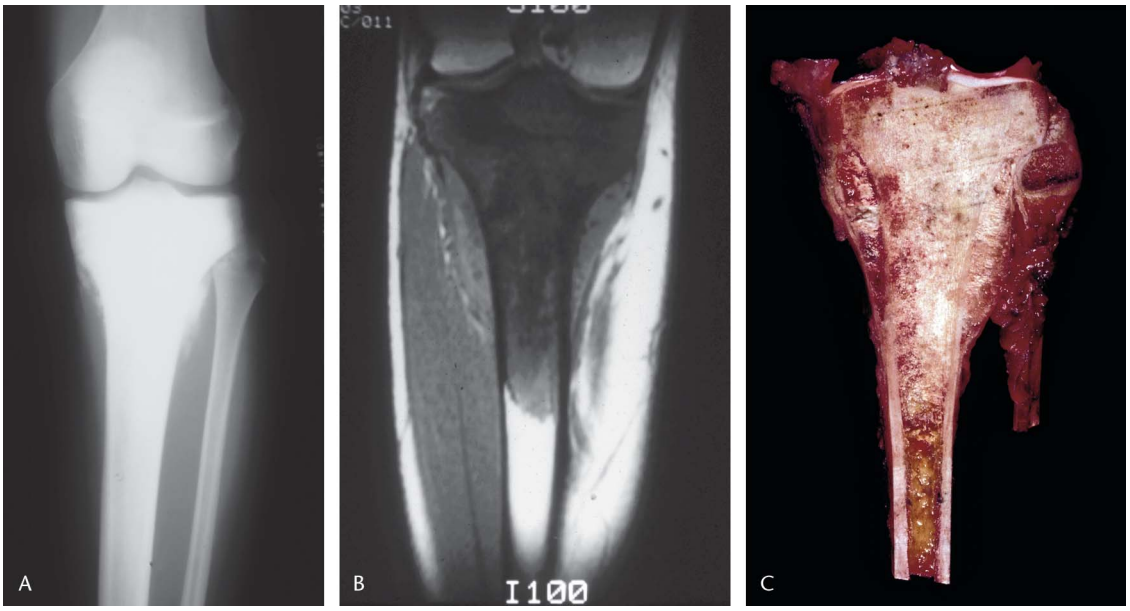

FIGURE 35. A–C, Seventeen-year-old male with osteosarcoma of the proximal tibia. Note that the lesion is radiodense, has a medial and lateral periosteal reaction with tumor bone, and that the margin of sclerosis is indistinct distally (A). A coronal MRI of the same lesion shows a fairly sharp interface of the lesion (compact bone and ossified tumor bone are both hypointense, or black on MRI in all studies) and the marrow fat (B). Following chemotherapy, the lesion was resected with a margin of several centimeters, allowing for an internal prosthesis rather than requiring an amputation. Note how the black areas of the MRI study correspond to the white tumoral areas of the gross specimen (C).

The smaller the nucleus, the less radiofrequency energy is required to induce magnetic resonance. For all practical purposes, the resonance signal measured using magnetic fields of the strength commonly used in medical applications is that of hydrogen atoms. This means that substances containing fat and free water resonate most freely. Interpreting MRI in simple diagnostic fashion does not require that a physician need understand all the subtle physical principles of MRI any more than driving an automobile requires one to be a mechanic. What is required is a general knowledge of anatomy combined with an awareness of the typical signals generated by various tissues in MRI (Figs. 33A–D and Table 1).

Whereas the spatial resolution of images in MRI is inferior to that in CT scans, this is likely to improve with technological advancements.[24] On the other hand, the degree of contrast is much better in MRI than in CT[25]; fat and water-containing objects contrast with one another in ways that are not appreciated on CT scans. Objects with little free hydrogen, such as compact bone (water of hydration in the crystalline hydroxyapatite lattice is not free hydrogen and is silent) do not

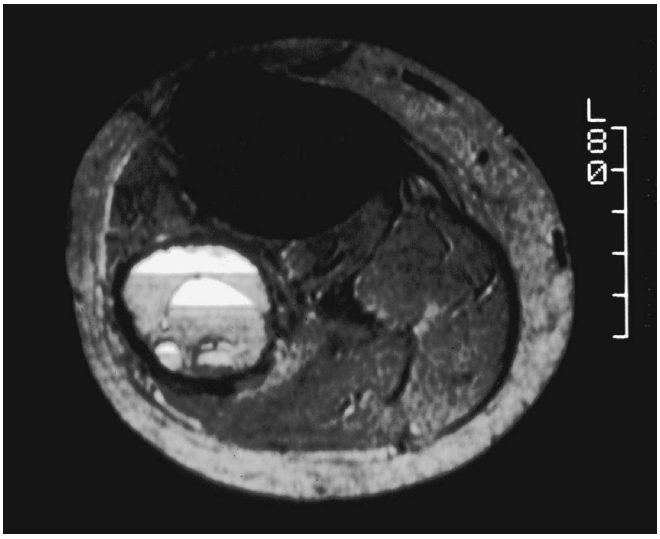

FIGURE 36. T_2 weighted image of aneurysmal bone cyst previously shown in Figure 18. The patient has been motionless in the scanner for over 40 minutes at the time this image is made. Note that the lobules comprising this lesion contain material with two different signal intensities. The lighter intensity on the top represents plasma, whereas the darker intensity on the bottom represents plasma that contains erythrocytes, which are in the process of settling. As the patient remains motionless, the constant mixing of the cellular and fluid elements and presumably the slow venous return that accompanies motion do not take place. The erythrocytes do not generate a signal, and the more compact the lower portion becomes, the darker this portion will be relative to the plasma on top. The resulting sign is called a fluid-fluid level, and it can form any place whole unclotted blood can settle. Theoretically, MRI could be used in a very expensive way to approximate a hematocrit in a person with ABC; it does tell us that the movement of blood in an intact aneurysmal bone cyst is very slow indeed.

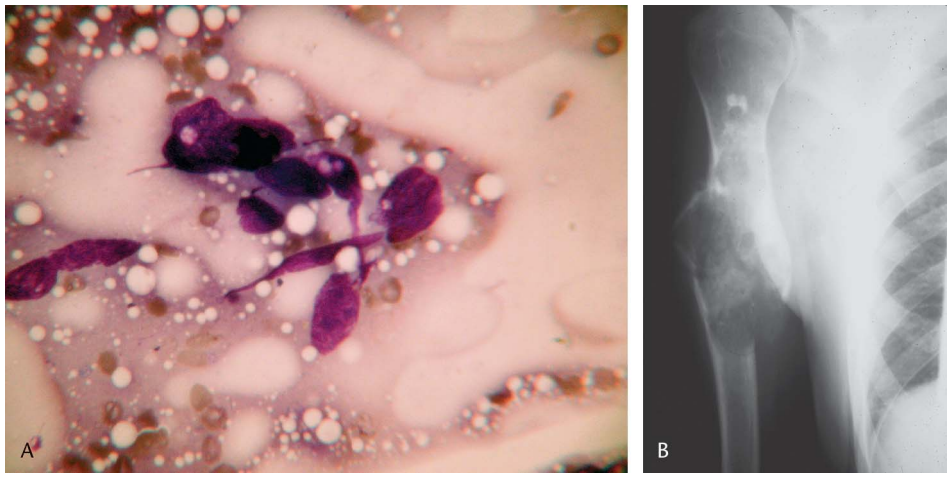

FIGURE 37. A, Fine needle aspiration of a lesion from the proximal humerus of a 57-year-old male sent to the author in consultation. The referring pathologist recognized the sarcomatous appearance of these cells and suggested a diagnosis of osteosarcoma (A). Whereas this diagnosis is cogent from a cytologic standpoint, it makes no sense clinically, because the patient is too old to develop osteosarcoma unless there was underlying Paget disease or previous radiation to the site. Because neither of these were in the history, the diagnosis would have been extraordinary. The referring pathologist obtained one A-P radiograph (B) that solved the problem. In addition to a radiolucent lesion with a pathologic fracture, the lesion demonstrated internal scalloping of the cortex and a radiolucent background containing radiodense rings, popcorn, and stippled densities diagnostic for calcification of cartilage matrix. Whereas a diagnosis of chondrosarcoma made perfect sense in a patient of this age, the referring pathologist pointed out that there were no chondrocytes obtained. The only correlation that made sense to the author was that a chondrosarcoma had undergone dedifferentiation to a higher grade sarcoma and that the more malignant component had in fact been sampled. The proximal humerus was excised and this proved to be the case.

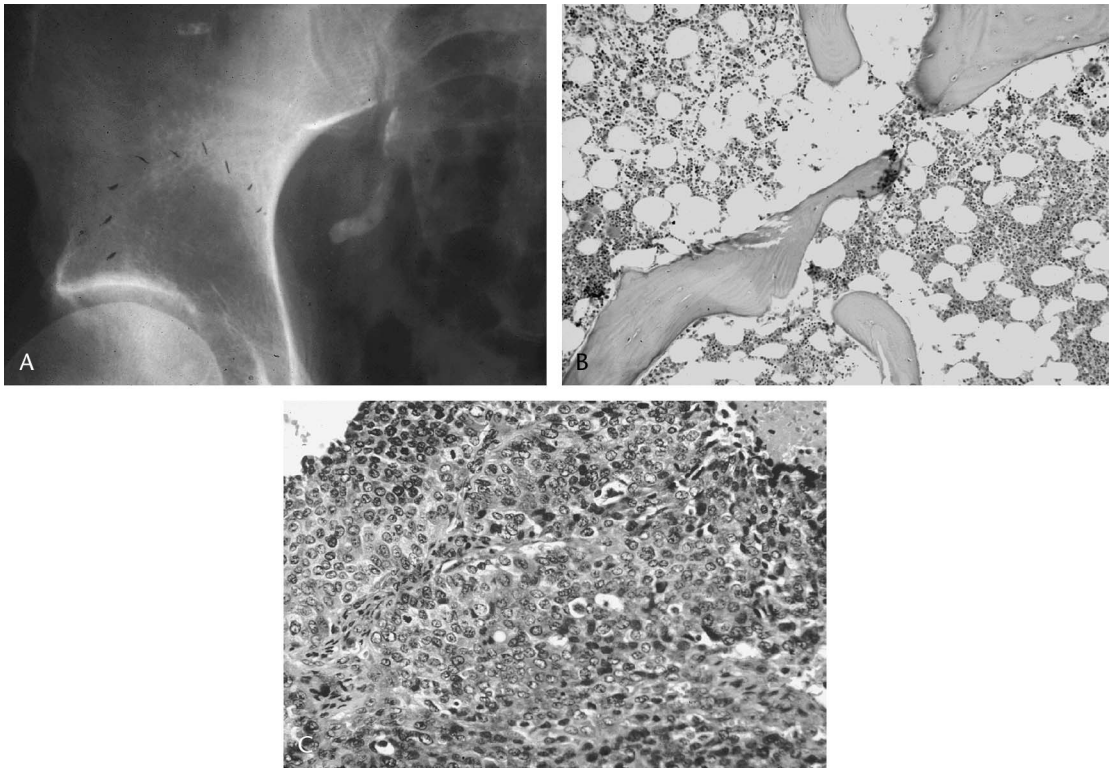

FIGURE 38. A–C, A 63-year-old man with a diagnosis of non small-cell lung carcinoma 6 months previously complained of severe right hip pain of recent onset. A conventional radiograph demonstrated a large radiolucent supra-acetabular lesion and the clinical diagnosis of metastatic carcinoma was made (A). The lesion was biopsied, but everything in the biopsy fragments looked like normocellular hematopoietic marrow and mature cancellous bone (B). Because a bone lesion would have to replace at least 40% of the bone at this site to cause a lesion to be visible radiographically and everything sampled showed no tumor, it was suggested to the surgeon that the biopsy had not obtained representative tissue. The surgeon sent the patient to a radiologist who sampled the lesion with a needle under CT guidance. The tissue (C), which demonstrated metastatic carcinoma, gives a great understanding of why it is important to interpret radiographs before we simply say ''no tumor is identified.''

give off a signal.[21] Because brightness is proportional to the resonance signal, cortical bone always appears dark. Whereas cancellous bone itself also gives off no signal, the medulla of the ends of bone is only 25% bone and 75% fat and marrow by volume. Because this fat gives off a strong signal, the medullary cavity appears bright.

The marrow in long bones is almost entirely fat and the marrow in flat bones also contains hematopoietic marrow, so the signal from fatty and hematopoietic marrow differs depending upon the particular MRI study technique used (Figs. 34A and 34B). Evaluation of the extent of soft tissue masses and of the interface of tumors with normal marrow is particularly superior on MRI (Figs. 35A–C). Because MRI can discriminate between water, fat, and whole blood, it can sometimes reveal physiological information about a dynamic process in the same way as scintigraphy (Fig. 36).

It can be appreciated from this short discussion that MRI and CT scanning are complementary studies. Whereas each is good at refining the sensitivity of information not obtainable by ordinary radiographs, CT scanning better obtains certain information and MRI is better at elucidating other information.

CONCLUSION

In summary, radiographic imaging often adds the critical information that puts bone biopsies into a rational reference frame. The presence of adequate imaging data can make even very scanty biopsies interpretable so long as a small number of diagnostic cells or a meager amount of tissue is obtained (Figs. 37A and 37B). Without the context of the clinical picture, even a fairly large amount of tissue is meaningless unless it happens to be histologically diagnostic (Figs. 38A–C). Certain diseases are so characteristic radiographically that they are practically diagnostic by imaging alone. Whereas other diseases are not quite so characteristic, properly performed imaging studies can help to arrange the differential diagnostic likelihood of lesions in a logical and hierarchal order. However, imaging analyses are seldom pathognomonic. Without biopsy confirmation, the imaging data from most lesions yields diagnostic probabilities, which regardless of their confidence limits will always have outliers. The ability to use imaging data as an adjunct in orthopedic pathology reduces the number of outliers, and in doing so makes pathologists more effective at their tasks.

REFERENCES

1. Jaffe HL. *Tumors and Tumorous Diseases of Bones and Joints*. New York, NY: Lea and Febiger; 1958.
2. Dorfman HD, Czerniak B. *Bone Tumors*. St. Louis, MO: Mosby; 1998.
3. McCarthy EF, Frassica F. *Pathology of Bone and Joint Disorders with Clinical and Radiographic Correlation*. Philadelphia, PA: WB Saunders; 1998.
4. Rutherford E. The Scattering of Alpha and Beta Particles and the Structure of the Atom. Phil Mag Ser 6, xxi 621–629; 1911.
5. Glucksman WJ, Coyner KB. General orthopedic radiology: radiography, arthrography, tomography, myelography, and diskography. In: Fitzgerald RH, Kaufer H, Malkani AL eds. *Orthopaedics*. St. Louis, MO: Mosby; 2002:37–48.
6. Novelline RA. *Squire's Fundamentals of Roentgenology*. 6th ed. Boston: Harvard Press; 2004.
7. Fechner R, Mills S. Tumors of the bones and joints. In: *Atlas of Tumor Pathology*, Third Series, Fascicle 8. Armed Forces Institute of Pathology; Washington, DC; 1993.
8. Sweet DE, Madewell JE, Ragsdale BD. Radiologic and pathologic analysis of solitary bone lesions. Part III: Matrix patterns. *Radiol Clin North Am*. 1981;19:785–814.
9. Sprawls Perry. *The Physical Principles of Diagnostic Radiology*. Baltimore, MD: University Park Press; 1977.
10. Spjut HJ, Dorfman HD, Fechner RE, et al. Tumors of bone and cartilage. In: *Atlas of Tumor Pathology*, Fascicle 5, Series 2. Armed Forces Institute of Pathology; Washington, DC: 1971.
11. Milch RA, Changus GW. Response of bone to tumor invasion. *Cancer*. 1956;9:340–351.
12. Greenspan A, Klein MJ. Radiology and pathology of bone tumors. In: *Musculoskeletal Oncology: An Interdisciplinary Approach*. Philadelphia, PA: WB Saunders Co.; 1992:13–72.
13. Lodwick GS. Predictor variables in bone tumors. *Semin Radiol*. 1966;1: 293.
14. Lodwick GS, Wilson AJ, Farrell C, et al. Determining growth rates of focal lesions of bone from radiographs. *Radiology*. 1980;134:577.
15. Madewell JE, Ragsdale BD, Sweet DE. Radiologic and pathologic analysis of solitary bone lesions. Part I. Internal margins. *Radiol Clin North Am*. 1981;19:715–748.
16. Ragsdale BD, Madewell JE, Sweet DE. Radiologic and pathologic analysis of solitary bone lesions. Part II: Periosteal reactions. *Radiol Clin North Am*. 1981;19:749–783.
17. Klein MJ. Pathophysiology of bone tumors. In: Fitzgerald RH, Kaufer H, Malkani AL, eds. *Orthopaedics*. St. Louis, MO: Mosby; 2002:991–1001.
18. Abdelwahab IF, Klein MJ, Kenan S, et al. Coexistence of primary bone tumors: report of 4 cases of collision tumors. *J Appl Commun Res*. 2002; 53:296–302.
19. Palestro CJ, Tomas MB. Nuclear medicine. In: Fitzgerald RH, Kaufer H, Malkani AL, eds. *Orthopaedics*. St. Louis, MO: Mosby; 2002: 64–70.
20. Kahn LB, Wood FW, Ackerman LV. Fracture callus associated with benign and malignant bone lesions and mimicking osteosarcoma. *Am J Clin Pathol*. 1969;52:14–24.
21. Olendorf W, Olendorf W Jr. *MRI Primer*. New York, NY: Raven Press; 1991.
22. Mitchell DG, Cohen MS. *MRI Principles*. Philadelphia, PA: Saunders; 2004.
23. Webb A. *Introduction to Biomedical Imaging*. Piscataway, NJ: IEEE Press-Wiley Interscience; 2003.
24. McLeod RA, Berquist TH. Bone tumor imaging: contribution of CT and MRI. In: Unni KK, ed. *Bone Tumors*. New York, NY: Churchill Livingstone; 1988:1–34.
25. Gilkey F, Sweet DE, Mirra J. Radiologic/pathologic correlation of bone tumors. In: Mirra J, ed. *Bone Tumors, Clinical, Radiologic, and Pathologic Correlations*. 2nd ed. Chapter 27. JB Lippincott Co.: Philadelphia, PA; 1989:1803–1831.
26. Sprawls Perry. *The Physical Principles of Diagnostic Imaging*. Baltimore, MD: University Park Press.

